

Climate Change Effects on Rainfall Intensity-Duration-Frequency (IDF) Curves for the
Town of Willoughby (HUC-12) Watershed Using Various Climate Models

by

Samir Mainali

Submitted in Partial Fulfillment of the Requirements

for the Degree of

Master of Science in Engineering

in the

Civil and Environmental Engineering Program

YOUNGSTOWN STATE UNIVERSITY

August 2023

Climate Change Effects on Rainfall Intensity-Duration-Frequency (IDF) Curves for the
Town of Willoughby (HUC-12) Watershed Using Various Climate Models

Samir Mainali

I hereby release this thesis to the public. I understand that this thesis will be made available from the OhioLINK ETD Center and the Maag Library Circulation Desk for public access. I also authorize the University or other individuals to make copies of this thesis as needed for scholarly research.

Signature:

Samir Mainali, Student Date

Approvals:

Dr. Suresh Sharma, Thesis Advisor Date

Dr. Sahar Ehsani, Committee Member Date

Dr. John W DeSantis, Committee Member Date

Dr. Salvatore A. Sanders, Dean of Graduate Studies Date

ABSTRACT

Climate change due to anthropogenic influences such as greenhouse gas emissions has been a pressing problem for the existing water resource infrastructure. The intensity and frequency of extreme precipitation have increased across various parts of the world and are expected to increase further by the end of the 21st century. Consequently, more frequent storm sewer flooding is likely to be experienced in future decades, leading to property damage, disrupting transportation and other services, and putting inhabitants at risk of flooding. Since heavy rains can trigger flash floods, there is a critical need to account for these anticipated shifts in precipitation patterns when planning for flood risk management and building resilient infrastructure in the Town of Willoughby (Hydrologic Unit Code, HUC-12) of the Lake Erie Basin.

The goal of this research is to derive insightful information on the potential impacts of climate change on the Town of Willoughby's water resources to take mitigation measures and minimize such impacts. The study employed observed historical data from Hopkins International Airport and the output of regional climate models (RCMs) and general circulation models (GCMs) from the Coupled Model Intercomparison Projects (CMIPs) Phases 5 and 6. The quantile mapping method was utilized to correct for biases in the CMIP data, and the Gumbel Extreme Value Type-I distribution was used to reflect the excessive rainfall occurrences for the Town of Willoughby. From CMIP5, three models were used in the analysis, and only one scenario, Representative Concentration Pathways (RCP) 8.5, was considered. For CMIP6, three models were selected, and four different scenarios were incorporated into the study, namely, Shared Socioeconomic Pathways (SSP), ssp126, ssp245, ssp370, and ssp585. Finally, intensity duration frequency (IDF) curves were

developed using various climate models and scenarios, analyzing them for a series of durations and return periods to investigate the impacts of changes in the climate on precipitation patterns.

The findings showed that even for 2-year return periods, the worst-case scenario for both RCP8.5 and SSP585 under CMIP Phase 5 and Phase 6, respectively, could have an impact on the current water management system with an increase in hourly precipitation intensity ranging from 9 to 26%, whereas the 100-year return period showed an increase in the range of 16 to 46%. The multi-model ensemble (MME) approach of both CMIP models for the worst-case scenario, i.e., RCP8.5 and SSP585, showed a rise in precipitation intensity of 9% to 39% in the near future (2020-2059) and 20% to 55% in the far future (2060-2099), depending on the various rainfall durations and return periods. The RCP8.5 scenario under CMIP5 models predicted a higher intensity of rainfall (up to 28% depending on the return period and rainfall durations) than the scenario SSP585 under CMIP6 models. The analysis of the various SSP scenarios (SSP126, SSP245, and SSP370) from CMIP6 has predicted an increase of 2-22% in the near future and 6-40% in the far future, with SSP126 showing the lowest increase and SSP245 and SSP370 following the increasing order.

This finding highlights the risk of extreme precipitation and recommends coordinated efforts by policymakers and planners to determine the most comprehensive approach to water management and infrastructure. This is critical to endure and adapt to the effects of climate change and ensure resilient infrastructure for future extreme rainfall events. In conclusion, this study focuses on the need for revised IDF curves to better manage the risks connected with climate change and its possible effects on the Town of Willoughby's water resources. Engineers, policymakers, and any other individuals might use the future IDF

curves generated in this study as a vital tool in mitigating the risks associated with extreme precipitation events.

Keywords: General Circulation Models (GCMs); Coupled Model Inter-Comparison Project (CMIP); Quantile Mapping; Bias Correct; Gumbel Extreme Value Type-I Distribution

ACKNOWLEDGEMENTS

I'd like to thank my advisor, Dr. Suresh Sharma, for his incredible assistance and unwavering support throughout the entirety of my thesis. Dr. Sharma's expert guidance and wealth of knowledge have played a pivotal role in my growth as a researcher, and I am immensely grateful for the time and effort he has dedicated to my development. In addition, I would like to express my sincere admiration for Dr. Sahar Ehsani and John W. DeSantis for their insightful suggestions and feedback. Their expertise and mentorship have proven invaluable, and I am truly appreciative for their contributions to my research. Furthermore, I would like to express my sincere appreciation to Dr. Anawarul Islam, the program coordinator, and Dr. Frank Li, the department chair, for their guidance and assistance throughout my academic journey.

I am also indebted to Youngstown State University for providing me with funding support, an enriching learning experience, and a conducive research environment throughout my study period. I would like to thank Ms. Linda Adovasio for her assistance and support during my research and studies.

To my colleagues in the department, I am deeply grateful for their contributions to both my professional and personal growth at YSU, as well as their encouragement at various stages of my research and thesis writing.

Finally, I wish to convey my heartfelt appreciation to my father, Rajesh Kumar Mainali, my mother, Shanta Mainali, and my wife, Prativa Pokhrel, for their unwavering love and support throughout my education and life. Their constant encouragement and belief in my abilities have been the driving forces behind my achievements.

TABLE OF CONTENTS

ABSTRACT	III
ACKNOWLEDGEMENTS	VI
LIST OF FIGURES.....	VIII
LIST OF TABLES	X
LIST OF ABBREVIATIONS	XI
Chapter 1: Introduction	1
Chapter 2: Climate Change Effects on Rainfall Intensity-Duration-Frequency (IDF) Curves for the Town of Willoughby (HUC-12) Watershed Using Various Climate Models.....	8
Chapter 3: Recommendations	57

LIST OF FIGURES

Figure 1. Location map of the study area showing Town of Willoughby, Ohio, USA ...	49
Figure 2. IDF curves for the baseline period (TS-1: 1980-2019) vs. the near future (TS-2: 2020-2059) considering a 2, 5, 10, 25, 50, and 100-year return period ensembling three CMIP5 RCP8.5 models.....	50
Figure 3. IDF curves for the baseline period (TS-1: 1980-2019) vs. the far future (TS-3: 2060-2099) considering a 2, 5, 10, 25, 50, and 100-year return period ensembling three CMIP5 RCP8.5 models.....	50
Figure 4. Graphical comparison showing the rainfall intensity percentage change between the baseline period (TS-1: 1980-2019) vs. the near future (TS-2: 2020-2059), on the left, and the baseline period (TS-1: 1980-2019) vs. the far future (TS-3: 2060-2099), on the right, for different return periods and rainfall durations of CMIP5 RCP8.5	51
Figure 5. IDF curves for the baseline period (TS-1: 1980-2019) vs. the near future (TS-2: 2020-2059) considering a 2, 5, 10, 25, 50, and 100-year return period ensembling three CMIP6 SSP126 models.....	51
Figure 6. IDF curves for the baseline period (TS-1: 1980-2019) vs. the far future (TS-3: 2060-2099) considering a 2, 5, 10, 25, 50, and 100-year return period ensembling three CMIP6 SSP126 models	52
Figure 7. IDF curves for the baseline period (TS-1: 1980-2019) vs. the near future (TS-2: 2020-2059) considering a 2, 5, 10, 25, 50, and 100-year return period ensembling three CMIP6 SSP245 models.....	52
Figure 8. IDF curves for the baseline period (TS-1: 1980-2019) vs. the far future (TS-3: 2060-2099) considering a 2, 5, 10, 25, 50, and 100-year return period ensembling three CMIP6 SSP245 models	53
Figure 9. IDF curves for the baseline period (TS-1: 1980-2019) vs. the near future (TS-2: 2020-2059) considering a 2, 5, 10, 25, 50, and 100-year return period ensembling three CMIP6 SSP370 models.....	53
Figure 10. IDF curves for the baseline period (TS-1: 1980-2019) vs. the far future (TS-3: 2060-2099) considering a 2, 5, 10, 25, 50, and 100-year return period ensembling three CMIP6 SSP370 models	54
Figure 11. IDF curves for the baseline period (TS-1: 1980-2019) vs. the near future (TS-2: 2020-2059) considering a 2, 5, 10, 25, 50, and 100-year return period ensembling three CMIP6 SSP585 models.....	54
Figure 12. IDF curves for the baseline period (TS-1: 1980-2019) vs. the far future (TS-3: 2060-2099) considering a 2, 5, 10, 25, 50, and 100-year return period ensembling three CMIP6 SSP585 models	55
Figure 13. Graphical comparison showing the rainfall intensity percentage change between the baseline period (TS-1: 1980-2019) vs. the near future (TS-2: 2020-2059), on	

the left, and the baseline period (TS-1: 1980–2019) vs. the far future (TS-3: 2060–2099), on the right, for different return periods and rainfall duration of CMIP6 SSP585	55
Figure 14. IDF curves for the near future period (TS-2: 2020–2059) considering a 2, 5, 10, 25, 50, and 100-year return period ensembling three CMIP5 RCP8.5 vs. CMIP6 SSP585 models	56
Figure 15. IDF curves for the far future period (TS-3: 2060–2099) considering a 2, 5, 10, 25, 50, and 100-year return period ensembling three CMIP5 RCP8.5 vs. CMIP6 SSP585 models	56

LIST OF TABLES

Table 1. Description of the climate models and climate change scenarios used in the study.....	47
Table 2. Bias in terms of mean and standard deviation (St. Dev.) before and after bias correction for CMIP5 and CMIP6 models for the baseline period (TS-1: 1980-2019)....	48

LIST OF ABBREVIATIONS

CDBC	Climate Data Bias Corrector
CMIP	Coupled Model Intercomparison Project
GCM	General Circulation Model
HUC	Hydrologic Unit Code
IDF	Intensity Duration Frequency
IPCC	Intergovernmental Panel on Climate Change
MME	Multi-Model Ensemble
NA-CORDEX	North American Coordinated Regional Downscaling Experiment
NOAA	National Oceanic and Atmospheric Administration
NRCS	National Resources Conservation Services
RCM	Regional Climate Model
RCP	Representative Concentration Pathways
SCS	Soil Conservation Service
SSP	Shared Socioeconomic Pathways
TS	Time Span
WCRP	World Climate Research Program

Chapter 1: Introduction

Over the last few decades, climate change studies have become a topic of research interest for water resources engineers and climatologists. The frequency of extreme precipitation occurrences has indicated an increasing frequency globally (Du et al., 2022; Martel & Mailhot, 2018) and regionally (Berg et al., 2013; Groisman et al., 2005a; Kourtis & Tsihrintzis, 2022a; Madsen et al., 2009a). More frequent extreme rainfall occurrences have been documented in numerous studies in the United States (Gershunov & Cayan, 2003; Karl et al., 1995; Karl & Knight, 1998), Australia (Sun et al., 2014; Westra et al., 2015), India (R. Zhang & Delworth, 2006), Europe (Cioffi et al., 2015), and China (Zhai et al., 2005). Ground-based observations conducted in the U.S. reveal a substantial surge in extreme rainfall events over the course of the last century (Degaetano, 2009; Hao et al., 2013; Kunkel et al., 2013; Thomas R. Karl et al., 2009). The Intergovernmental Panel on Climate Change (IPCC) Assessment Report (IPCC, 2007) found that trends in extreme precipitation are very likely to maintain an upward trajectory after using a range of general circulation models (GCMs) to estimate future climate with different emission scenarios.

Urban drainage design entirely relies on the intensity duration frequency (IDF) curve as a fundamental tool for managing precipitation and flooding (Guo & Asce, 2006a). IDF curves are often used in the engineering design fields of municipal stormwater management and other areas across the world (Endreny & Imbeah, 2009; Haddad et al., 2011; Madsen et al., 2002, 2009b; Willems, 2013a). Therefore, it is critical to review and update rainfall characteristics for future climate scenarios (Cook et al., 2020a; L. Liu, 2023a; Martel et al., 2021a; Mirhosseini et al., 2013). Statistical evaluations of historical data have traditionally been used in the development of drainage systems with the assumption that the intensity

and frequency of past events are a fair representation of what could occur in the future (Grum et al., 2006; He et al., 2006; Papa et al., 2004). Since climate change is projected to affect the frequency and intensity of extreme precipitation events, it is important to examine this hypothesis and adjust during the design of the drainage infrastructure (Mailhot et al., 2006). Several efforts have been made to promote the design of hydraulic infrastructure that is resilient to climate change and to consider nonstationary factors in the analysis of IDF curves (Cheng & Aghakouchak, 2014a; Noor et al., 2018, 2022; Ouarda et al., 2019; Yan et al., 2019; Yilmaz & Perera, 2014).

The evaluation of precipitation data is essential for the management of water resources, flood forecasting, and informed decision-making processes for operational warnings, as rainfall is a significant climate factor that impacts the spatial and temporal distribution of water availability (Debbage & Marshall Shepherd, 2019; S. Liu et al., 2018; Tiwari et al., 2020; Weldegerima et al., 2018). Due to the limitation of sub-daily data, most research evaluating the impact of extreme events in the US relies on the analysis of daily rainfall data (Cook et al., 2020b; Z. Li et al., 2019; Moraglia et al., 2022; Sohoulane Djebou et al., 2021; Sowby & Capener, 2023; Statkewicz et al., 2021; Weathers et al., 2023; N. Zhang et al., 2019). Daily resolution is still extensively used for monitoring precipitation, although it is not ideal for measuring alterations in extreme occurrences because most of these occurrences last on a sub-daily and sub-hourly scale (Barbero et al., 2019; Meira et al., 2022; Morrison et al., 2019; Pui et al., 2012). Because the peak inundation value heavily relies on the temporal precision of the storm input, flood simulation models benefit from the use of sub-daily rainfall data as opposed to daily data (Bruni et al., 2015; Hou et al., 2020; Huang et al., 2019), and sub-daily data has a higher resolution, unique statistical

traits and displays different spatial and temporal patterns of variability when compared to data that is aggregated on a daily basis (Trenberth & Zhang, 2018).

Despite the growing concern, there has been limited research on evaluating changes in precipitation intensity, duration, and frequency in a nonstationary climate, particularly in the great lake regions, especially on an hourly scale, where the lake effect leads to unique precipitation patterns and variations.

Climate models and scenarios

The increase in greenhouse gas emissions into the Earth's atmosphere, such as carbon dioxide (CO₂) and methane (CH₄), is the main cause of climate change. These emissions come from various human activities, including the burning of fossil fuels for energy, deforestation, and industrial processes. The accumulation of these greenhouse gases traps heat in the atmosphere, leading to a rise in global temperatures and changes in climate patterns. To understand and project the impacts of climate change, the IPCC plays a vital role.

The IPCC assesses scientific research and provides comprehensive reports on the state of the climate system, potential risks, and possible mitigation strategies. The IPCC relies on GCMs to simulate future climate scenarios. Two major phases of these models are CMIP (Coupled Model Intercomparison Project), Phase 5, and Phase 6. CMIP5 and CMIP6 involve a collection of climate models that simulate the Earth's climate system. CMIP5 used Representative Concentration Pathways (RCPs) to estimate future greenhouse gas concentrations, while CMIP6 incorporates Shared Socioeconomic Pathways (SSPs)

alongside RCP scenarios. The IPCC utilizes these models and scenarios to project the rise in global temperatures under different emission pathways.

CMIP6 improves upon CMIP5 by including SSPs in addition to the RCPs utilized in CMIP5. CMIP5 relied on four RCPs to define future greenhouse gas concentration scenarios, while CMIP6 integrates qualitative and quantitative components through SSPs, considering factors such as demographics, human development, policies, and natural resources. This evolution enhances the robustness and significance of future climate projections, providing a more comprehensive understanding of potential climate conditions. Overall, CMIP6 is an extension and enhancement of the modeling strategy that makes climate models more accurate and practical. CMIP6's SSPs cover a wide variety of potential futures. SSP126 represents a sustainability-focused pathway with strong mitigation efforts aiming to limit global warming to well below 2 degrees Celsius by the end of the century. SSP245 represents an intermediate emissions pathway with moderate socio-economic development and emission reduction efforts. SSP370 portrays a scenario of fragmented global development where regions prioritize their own interests, resulting in higher greenhouse gas emissions. Lastly, SSP585 illustrates a high-emission route, showing a prolonged dependence on fossil fuels and inadequate climate mitigation initiatives. These diverse scenarios capture a spectrum of possible future trajectories, allowing for a comprehensive assessment of the potential impacts of different socio-economic and emission pathways on climate change.

Therefore, this study aimed to assess the effect of climate change on IDF curves and the occurrence of extremes using the latest CMIP Phase 6 as well as the preceding version, Phase 5, on a sub-daily scale. Since the comparison of both CMIP5 and CMIP6 models for

IDF curve development has been limited, specifically exploring this aspect in the US or the Lake Erie basin has not been reported. Additionally, the comparison of the IDF curve from the output of CMIP Phase 5 and 6 models using various emissions has been reported.

Scope and objectives

The following are the key objectives of this research study:

- I. To estimate the IDF curve for the Town of Willoughby (HUC-12) using both CMIP5 and CMIP6 models under various climate change scenarios.
- II. To compare and assess the differences in the anticipated precipitation IDF curves between CMIP5 RCP8.5 and CMIP6 SSP585.

Methodology for Objective I

- a) Collect hourly climate data, including historical observations from the National Oceanic and Atmospheric Administration (NOAA) and climate models using CMIP 5 and 6;
- b) Correct the bias of the climate data obtained from the climate models using the observed historical data using the Climate Data Bias Corrector (CDBC);
- c) Compute the extreme precipitation for different hours (1-hour, 2-hour, 6-hour, 12-hour, and 24-hour);
- d) Develop the IDF curve using the extreme precipitation data for a range of durations and return periods.

Methodology for Objective II

The steps for Objective I (a, b, and c) also apply to Objective II. The additional steps for Objective II are as follows:

- a) Construct the IDF curve using the extreme precipitation data for various durations and return periods for CMIP5 RCP8.5 and CMIP6 SSP585;
- b) Analysis of the IDF curves of both CMIP models and identify and report the disparities.

Thesis Structure

This thesis is structured into three chapters, with Chapter 1 providing an overview of the background, scope, and objectives of the thesis. Chapter 2 focuses on the bias correction of the climate data obtained from the climate models using the CDBC and calculates the extreme precipitation events for different hours using the Gumbel Extreme Value Type-I distribution. This chapter also explains in detail the theoretical background of the climate models, the quantile mapping methodology for bias correction, and the Gumbel Extreme Value Type-I distribution to accurately represent the extreme rainfall events in the Town of Willoughby. Additionally, it develops the IDF curves that take climate change into account and emphasizes the importance of IDF curves for engineers, who can use them to more accurately predict the peak flow and volumes of runoff that drainage structures will need to manage in various climate change scenarios. Furthermore, it describes the development of the hourly IDF curve for the Town of Willoughby under various scenarios, durations, and return periods, which is crucial for estimating the probability of precipitation events with varying intensity and duration.

In Chapter 3, the conclusions drawn from this study and the recommendations for future research to enhance the development of IDF curves under climate change for more effective and resilient drainage structures have been discussed. Chapter 2 has been structured in journal paper format and will be developed into a full-length article after incorporating additional work in the future. As a journal article should be self-contained and provide adequate background information, readers may encounter some repetitive content in this chapter.

Chapter 2: Climate Change Effects on Rainfall Intensity-Duration-Frequency (IDF) Curves for the Town of Willoughby (HUC-12) Watershed Using Various Climate Models

Abstract

Changes in precipitation patterns due to climate change are projected to have profound effects on several hydrological processes. The anticipated shifts in the intensity-duration-frequency (IDF) relationship have an impact on the design of water infrastructure as well. Consequently, it is crucial to understand the potential changes to the IDF to manage and adapt to climate change's implications on water resources. This study delves into the analysis of hourly observed as well as future precipitation data in the Town of Willoughby (HUC-12) to examine the variations in IDF relationships over the 21st century. To accomplish this, several regional climate models (RCMs) and general circulation models (GCMs) from the Coupled Model Intercomparison Project (CMIP) Phases 5 and 6 were used. The study evaluated three RCMs with historical and Representative Concentration Pathway (RCP) 8.5 scenarios for each CMIP5 and three GCMs with historical and Shared Socioeconomic Pathways (SSP) (126, 245, 370, and 585) scenarios for each CMIP6. The quantile mapping methodology was used to adjust the biases in the data extracted from the CMIP models, while the Gumbel Extreme Value Type-I distribution was chosen to accurately represent the extreme rainfall events in the Town of Willoughby. The results suggest that the Town of Willoughby will experience an increase of 9–46% in the hourly precipitation intensity under the worst-case scenarios of RCP8.5 for CMIP5 and SSP585 for CMIP6. This increase is expected to occur in both the near (2020–2059) and far future (2060–2099), with a return period as low as 2 years and as high as 100 years when

compared to the baseline period (1980–2019). The analysis suggests an increase range of 9–39% in the near future and 20–55% in the far future across various scenarios, return periods, and rainfall durations for CMIP5 RCP8.5 and CMIP6 SSP585. In contrast to CMIP6 SSP585 models, CMIP5 models predict rainfall with an intensity value that is up to 28% higher, both for return periods and rainfall duration. Furthermore, the findings demonstrate that under different scenarios of SSP126, SSP245, and SSP370 under CMIP6 models, rainfall intensity is predicted to increase with a range of 2–22% in the near future and 6–40% in the far future as compared to the baseline period. The findings of this study are expected to be helpful for the planning and design of hydraulic structures and urban water resource infrastructures in the context of a changing climate by utilizing the updated IDF relationships.

Key Words: General Circulation Models (GCM); Coupled Model Inter-Comparison Project (CMIP); Quantile Mapping; Bias Correct; Gumbel Extreme Value Type-I Distribution

Introduction

Future intensification of extreme precipitation events due to greenhouse gas emissions will result in an increase in the frequency and length of rainfall events worldwide (IPCC, 2021). Several studies have reported a significant rise in both total annual precipitation and the frequency of extreme events (Allen & Ingram, 2002; Swain et al., 2020; Tabari, 2020; Trenberth et al., 2003). More specifically, shorter-duration precipitation events are expected to increase significantly across the world (Haerter & Berg, 2009; Lenderink & Van Meijgaard, 2008). For example, hourly extreme precipitation events (Westra et al., 2014) are expected to advance up to 400% in North America (Prein et al., 2017). Similar trends can also be observed in the United States (Easterling et al., 2000; Groisman et al., 2005b, 2012; Kourtis & Tsihrintzis, 2022b). The Intergovernmental Panel on Climate Change (IPCC, 2014) also projects that over the 21st century, heavy precipitation will occur in this area more frequently and with greater intensity.

Future high-intensity rainfalls triggered by climate change will have a more detrimental effect on urban stormwater systems (Cook et al., 2020c; Thakali et al., 2016). Since rainfall characteristics, such as intensity-duration-frequency (IDF) curves, are frequently utilized to design water infrastructures, it is essential to gain a comprehensive understanding of the alterations in extreme precipitation and subsequently revise the IDF curves in the future (Guo & Asce, 2006b; L. Liu, 2023b; Martel et al., 2021b; Mirhosseini et al., 2013). The IDF curve has been extensively used across the world for the design of hydraulic structures including urban drainage, culverts, road bridges, and storm sewer systems (Abdulrasheed Mohammed et al., 2021; Elsebaie, 2012a; Kundwa, 2019; Rashid et al., 2012).

The pressing need to reexamine the IDF curve arises from potential changes in intense rainfall exacerbated by climate change (Singh et al., 2016). Some studies suggest that proactively anticipating design modifications for hydraulic structures would decrease the risk of future issues and uncertainties, resulting in successful and versatile project outcomes (Prodanovic & Simonovic, 2007; Srivastav et al., 2014). Many scientists and professionals have advocated for better knowledge of the possible change in the severity, frequency, and volume of intense rainfall due to climate change (Hess et al., 2008; Hosseinzadehtalaei et al., 2020; Peck et al., 2012a; Rodríguez et al., 2014; Trenberth, 2011). This understanding is necessary since the existing drainage systems and hydraulic infrastructures are built to handle historical rainfall time series data on the basis that past extremes can be used to describe future extremes. This presumption is incorrect given the shifting frequency and amount of intense rainfall triggered by changing climatic variables (Shrestha et al., 2017). With these changes, historic IDF curves cannot be used to accurately represent future climatic conditions. Therefore, a changing climate may result in an increase in demand that water management infrastructure built to previous IDF norms may not be able to accommodate (Peck et al., 2012b). Climate models that integrate greenhouse gas emissions have become increasingly accessible and within reach to foresee future changes in the IDF curve (Cook et al., 2020; Ghasemi Tousi et al., 2021; Lopez-Cantu et al., 2020).

To date, the climate models are the primary and most effective tools for past and future climate simulations (Chen et al., 2020). However, the prediction of the future climate is location-specific and varies depending on the type of general circulation models (GCMs) and the scenario chosen. For example, according to Coupled Model Intercomparison Project (CMIP) Phase 5 projections, the distribution of temperature and precipitation

indices in the north-eastern US will undergo significant changes between 2041 and 2070 (Thibeault & Seth, 2014). Ragno et al. (2018) found that densely populated places may experience up to 20% more intense and twice as frequent extreme precipitation events. Cheng & Aghakouchak (2014) found that the assumption of extreme precipitation in a stationary climate may lead to an underestimation of extreme precipitation of up to 60%. Coelho et al. (2022) conducted a study using CMIP6 projections to assess the impact of changing extreme precipitation on flood engineering design across the US. By 2100, the northern region is predicted to experience an increase of 10–40% and the southern region, 20–80%. The study showed a meridional dipole-like pattern in the geographical distribution of precipitation changes, with an increase of 10–30% over the US (Almazroui et al., 2021). The results from the CMIP6 models at Tucson, Arizona, show the likely threat of future extreme events being disregarded in stationary-based design frameworks could pose a significant risk to both safety and economy by more than 300% (Ghasemi Tousi et al., 2021).

Limited studies have been conducted using predicted precipitation from CMIP6 models in the US, and no future IDF curve has been developed in the Lake Erie Basin using CMIP5 and CMIP6 climate models. As the precipitation pattern of the Lake Erie basin is complex due to lake-enhanced precipitation and rainfall after the snowfall, the future IDF curve due to climate change impacts is crucial in the Lake Erie basin to safely design urban drainage infrastructure and other hydraulic structures. Since climate change effects are region-specific, site-specific evaluations are required to boost local resilience to future extreme precipitation events. As a result, the clear differences in the future IDF curve compared to the existing IDF curve developed based on the historical observed data are needed in order

to incorporate such information in urban drainage systems to design climate-resilient infrastructures to mitigate the possible hazardous impact of climate change on infrastructure. Therefore, the objective of this paper is twofold: i) to derive the future IDF curve for the Town of Willoughby (HUC-12) using both CMIP5 and CMIP6 models; and ii) to compare and evaluate the differences in the projected precipitation IDF curves between the two sets of models. The purpose of this paper is to give a thorough understanding of the vulnerabilities associated with future changes in precipitation patterns in the Town of Willoughby.

Theoretical Description

CMIP5 Data Set

Multiple Representative Concentration Pathways (RCP) experiments have been used with the North American Coordinated Regional Climate Downscaling Experiment (NA-CORDEX) and CMIP5 model data to build various meteorological information at the regional scale (Lee et al., 2014). The major benefit of NA-CORDEX is that it uses general circulation models (GCMs) to drive simulations of various regional climate models (RCMs) at higher resolutions (e.g., 50 x 50 km) (Rummukainen, 2016). Such information is critical for accurately modeling the climate of regions with complicated topography and small-scale events. The limitations of GCMs, i.e., coarser resolution (100 x 100 km), are often resolved by regional climate model-based projections (Park et al., 2013), further substantiating the assertion that RCMs are frequently used to address the shortcomings of GCMs. Using the Western US as an example, Qian et al. (2010) demonstrated how the

RCM reflects the actual spatial variability in precipitation and snowfall using regional climate simulations at 40 km spatial resolution for the period (2040-2060).

In places with complicated topography where small-scale phenomena are critical for accurately representing the region's climate, NA-CORDEX's use of GCMs to drive the simulations of several RCMs is a major advantage. The NA-CORDEX has provided simulated precipitation data for two periods, including historical (1980–2005) and future (2006–2099) for CMIP5.

CMIP6 Data Set

The primary objective of CMIP6 is to provide multi-model climate forecasts based on alternative scenarios that are influenced by a new set of emissions shared socioeconomic pathways (SSPs) and land use scenarios that are directly related to societal concerns about adaptation, mitigation, or the consequences of climate change (O'Neill et al., 2016). By standardizing socioeconomic and technical assumptions across models, this new paradigm closed crucial gaps in CMIP5's intermediate forcing levels and allowed for a more thorough examination of various pathways. The World Climate Research Program (WCRP) has provided simulated precipitation data for two periods, including historical (1980–2014) and future (2015–2099) for CMIP6.

NA-CORDEX and WCRP both have the goal of improving our understanding of the Earth's climate and its potential future changes (Giorgi et al., 2009; J. W. Gutowski et al., 2016; McGinnis & Mearns, 2021). While NA-CORDEX focuses on producing high-resolution climate projections specifically for North America, WCRP is broader in its focus, coordinating and conducting research on the fundamental science of the Earth's

climate system and its interactions with the environment globally (W. J. Gutowski et al., 2021; Kirtman & Pirani, 2009).

In addition to retaining the CMIP5 emission trajectories RCP2.6, RCP4.5, RCP6.0, and RCP8.5, the CMIP6 data also contains three brand-new emission paths: RCP1.9, RCP3.4, and RCP7.0. As a result, the new scenarios combine SSP1, SSP2, SSP3, SSP4, and SSP5 of five socioeconomic paths with various levels of emissions to form seven future SSP-RCP scenarios, which include SSP1-1.9 (a very low range of scenarios) to SSP5-8.5 (a combination of high societal vulnerability and a high forcing level). The combination of RCPs and shared socioeconomic pathways (SSPs) is expected to make future scenarios more realistic.

It is expected that CMIP6 simulations can reproduce historical climate variables, represent smaller biases in sea surface temperature, and be more skillful in capturing the precipitation pattern. The climate model simulations from CMIP6 seem to be more reliable than earlier CMIP5 in various aspects. Different scientists have reported the limitations of CMIP5, especially in various scenarios and GCM output, due to the large reduction in atmospheric aerosol emissions for RCP scenarios. Since more realistic results can be expected at various locations, especially for extreme precipitation, the application of the latest CMIP6 climate data is more crucial for storm sewer drainage systems. In addition, the multimodal median of CMIP6 (CMIP6-MMM) is expected to perform better than the individual model. Therefore, several models were used for IDF curve development.

Bias Correction

Before any form of analysis, it is crucial to retrieve the data from climate models like RCMs and GCMs for a specific location based on latitude and longitude. Since it is not unusual for climate models to produce frequently skewed results, it is necessary to adjust the climate data for bias. This bias correction is essential and is recommended in several studies (Bruyère et al., 2014; Donat et al., 2016; Xue-Jie et al., 2013) to ensure that the bias-corrected data used in hydrological modeling and decision-making processes are accurate and reliable, leading to appropriate results (Maraun et al., 2017; Mehrotra & Sharma, 2012; Xu & Yang, 2012).

Out of the several bias correction methods, the quantile mapping method is the most popular and widely used across the world (Acharya et al., 2013; Lafon et al., 2013; Wood et al., 2004a). Quantile mapping is a technique used to reconcile climate model data with historical observations by transforming the model's data distribution to match the observational data distribution, thereby reducing biases and increasing accuracy in climate predictions (Abatzoglou & Brown, 2012; J. Chen et al., 2013; Gudmundsson et al., 2012; Maraun, 2016; Maraun et al., 2010; Pierce et al., 2014; Tabari et al., 2021). The efficiency of this technique has been tested and found to be effective in improving accuracy for hydrological modeling and decision-making (Grose et al., 2011; Hayhoe et al., 2008; Maurer & Duffy, 2005; Wood et al., 2004b). Quantile mapping is well-known for bias correction for specific climate circumstances. The approach aims to closely mimic both the statistical distributions of the observed variable and the climatic variable (H. Li et al., 2010; Maurer & Pierce, 2014).

Intensity Duration Frequency Curves

In the 1940s, Gumbel developed the Gumbel distribution, also known as the extreme-value Type I distribution (Obaid et al., 2014). The Gumbel theory of distribution is the preferred choice for analyzing intense rainfall events due to its simplicity (AlHassoun, 2011; Hailegeorgis et al., 2013). The Gumbel method has been found to be one of the most credible approaches for hydraulic design, particularly when dealing with high-intensity events due to its focus on extreme occurrences. Several past studies have shown that Gumbel's distribution may reliably anticipate flood magnitudes, enhancing the safety of the design (Al Islam & Hasan, 2020; Elsebaie, 2012b; Mujere, 2011; Solomon & Prince, 2013; Vidal, 2014). Similarly, ISFRAM (2015, 2016) suggests the use of the Gumbel Method in practical applications due to its improved accuracy results compared to Log-Pearson Type III. Nonetheless, the Gumbel distribution was found to be the best fit for the Kelantan River Basin, outperforming the Log Pearson Type III and Normal distributions (Yong et al., 2021). It has been observed that the application of Gumbel distribution improves the efficient design and utilization of infrastructure facilities, resulting in improved public safety and cost savings (Solomon & Prince, 2013).

The following equation (Elsebaie, 2012) calculates the maximum precipitation P_T (in mm) for each duration with a specified return period T (in years).

$$P_T = P_{avg} + KS \quad (1)$$

where P_{avg} is the average of the maximum precipitation corresponding to a given duration, as stated by:

$$P_{avg} = \frac{1}{n} \sum_{i=0}^n P_i \quad (2)$$

where “ P_i ” is the specific extreme value of rainfall and “ n ” is the number of events or years of data available.

K is the Gumbel frequency factor as given by:

$$K = -\frac{\sqrt{6}}{\pi} + \left(0.5772 + \ln \left(\ln \left(\frac{T}{T-1}\right)\right)\right) \quad (3)$$

and S is the standard deviation, which is computed using Eq. (4):

$$S = \left[\frac{1}{n-1} \sum_{i=0}^n (P_i - P_{avg})^2 \right]^{1/2} \quad (4)$$

where S is the standard deviation. The frequency factor (K), when multiplied by the standard deviation, provides the deviation of a specific rainfall event (for a certain period T) from the average. The rainfall intensity (i) in mm/hr can then be calculated using this factor and the standard deviation, as follows:

$$I_t = \frac{P_T}{T_d} \quad (5)$$

where T_d is the duration in hours.

Materials and Methods

Study Area

The study was conducted in the town of Willoughby, located in Lake County, Ohio, USA. The city is situated at 41° 38′ 45″ N and 81° 24′ 35″ W and covers a total area of 26.78 km², with 26.55 km² being land and 0.23 km² being water.

The climate of Willoughby is characterized by hot, muggy summers with scattered clouds and cold, snowy, windy winters. The average annual temperature ranges from -5°C to 28°C , and it is rarely below -13°C or above 32°C . Rainfall is frequent throughout the year, with the wettest month being September, which averages 78.74 mm of rain, and the driest month being February, with an average of 27.94 mm of rain. These climate patterns have been carefully monitored and recorded from 2015 to 2023, giving us a comprehensive understanding of the distinctive features of Willoughby's weather (Weather Spark).

Historical climate data shows that the area has experienced an upsurge in temperature and rainfall intensity in recent years, and extreme weather events show upward trends in precipitation days into the future (Bartels et al., 2020). Figure 1 illustrates the geographical context of the study area.

Climate Model Data

Past observed precipitation as well as RCM and GCM output data for different models from CMIP5 and CMIP6, respectively, are included in the precipitation data used with historical data and future data under various scenarios. The closest stations at Cleveland Easterly (ID: COOP:331651) and Burton (ID: COOP:331113), which are respectively 20 km and 35 km from the study area, lacked sufficient data for the period of 1980–2019 due to gaps in data collection. Therefore, the historical observations were collected from the Hopkins International Airport station in Cleveland, Ohio, United States (ID: COOP:331657), which is 50 km away from the study site. The 1-hour precipitation data from the station was utilized to prepare the observed historical data. This station was

selected because it provides long records of continuous data sets without any significant interruption.

The historical period from 1980–2019 was considered the baseline period and referred to as Time Span-1 (TS-1), whereas the future period was divided into two time spans: 2020–2059 as the near future (TS-2), and 2060–2099 as the far future (TS-3). This was intended because the most recent data was available for the period of 1980–2019, and separating the future period into smaller time frames would allow for a more detailed analysis of potential changes in precipitation patterns with equal time for the near future and distant future, providing a more comprehensive and holistic view of the potential changes in precipitation patterns over time.

For this study, three RCMs with model-generated historical data and RCP8.5 scenarios for each CMIP5 were selected from <https://na-cordex.org/>. Similarly, for CMIP5, three GCMs with historical and four SSP scenarios—namely, SSP126, SSP245, SSP370, and SSP585—were chosen to examine the potential increase in future precipitation. The projected simulations of precipitation in the future were obtained from three climate models contributing to CMIP6: <https://esgf-node.llnl.gov/search/cmip6/>. The fundamental information for the three selected CMIP5 and CMIP6 models is reported in Table 1.

The ability of the climate models to contribute hourly data was a primary factor in their selection for this study. In addition, these models have already been widely adopted in the research community, ensuring comparability and consistency with existing literature and increasing the credibility and reliability of the research. Furthermore, a more nuanced comprehension of the potential effects of climate change on precipitation patterns was

made possible by including both historical and different future scenarios. Such climate scenarios help us understand how precipitation responds to changes in greenhouse gas emissions, which is useful for planning responses to climate change.

Bias correction of raw data

The climate data from the climate model are corrected in this study against the observed daily data using the quantile mapping bias-correction approach, also known as probability mapping or distribution mapping. For CMIP5 and CMIP6, the bias correction is continuously directed from 1980 to 2005 and from 1980 to 2014, respectively.

In this study, the Climate Data Bias Corrector (CDBC) tool developed by Gupta et al. (2019) was used to complete the bias correction. The effectiveness of the tool and its efficacy for bias corrections have been demonstrated in various studies (Ayugi et al., 2022; Babaousmail, Ayugi, et al., 2022; Babaousmail, Hou, et al., 2022; Lim Kam Sian et al., 2022; S. Shrestha et al., 2019).

Development of the IDF Curve

After the raw climate model data obtained has been bias corrected, the next step is to develop an IDF curve using the Gumbel Extreme Distribution method. For this, the raw data were analyzed to determine the maximum precipitation intensity for each year from 1980 to 2099 for different rainfall durations (1 hr, 2 hr, 6 hr, 12 hr, and 24 hr). In this study, the various return periods (including 2, 5, 10, 25, 50, and 100 years) were taken into consideration. For each return period, the intensity of precipitation for each duration was calculated using the average of the maximum precipitation and the standard deviation

corresponding to the time frame. In addition, the Gumbel frequency factor, or K-factor, was used to calculate the probability of the occurrence of an event of a given magnitude.

Finally, the IDF curve was developed by plotting the intensity of precipitation against the duration of the rainfall for each return period using the Multi-Model Ensemble (MME) mean method.

Results and Discussion

Since the major objective of this study was to develop IDF curves for both CMIP5 and CMIP6 models and evaluate the differences between them, simulated precipitation data for historical and future periods was used. The data was adjusted to reduce biases using the quantile mapping approach, and the results of the bias correction process are presented in terms of the mean and standard deviation. Table 2 illustrates the comparison of the average and variability (standard deviation) in both CMIP5 and CMIP6 models, both before and after bias correction.

CMIP5

A comprehensive analysis of the IDF curves, assembling three CMIP5 models for the RCP8.5 scenario, provides a visual and mathematical representation of the changes in IDF. The IDF curve for the TS-1 and the TS-2 is presented in Figure 2. The analysis has revealed a considerable rise in rainfall intensity in the TS-2 compared to the TS-1, with a projection of 9–39% for various durations and return periods. It is important to note that the percentage increase is not linear, with large increases seen for longer durations and higher return periods. The non-linear nature of the increase in rainfall intensity implies that extreme rainfall events are projected to become even more intense in TS-2. The analysis

of the trend of precipitation indicated that the increasing pattern observed in the TS-2 is expected to further increase in the TS-3, as shown in Figure 3. Precipitation is expected to become more intense and increase by 20–55% compared to TS-1. The occurrence of extreme rainfall events with both shorter and longer return periods has increased in terms of both frequency and intensity. This tendency raises concerns about the likelihood of more frequent flash floods and stormwater flooding in the future. To further illustrate this point, Figure 4 presents a graphical comparison of the percentage change in intensity between different time frames. The study reveals that until the final years of the century, hourly precipitation with a 100-year return period will increase by almost 24%. Hourly precipitation intensity is seen to follow a predictable trend, increasing by 16.15% in the TS-2 and by a much larger percentage (29.12%) in the TS-3. These divergent tendencies highlight the value of looking across multiple time periods when analyzing climate projections for the future, which provide important clues that help us piece together how precipitation patterns may shift over time. The increasing trend of precipitation in the Lake Erie region that we found in our study is consistent with the findings of previous research by Xue et al. (2022) and L. Zhang et al. (2020) on the Great Lakes region using CMIP5 models. Notably, the same models were used, which suggests the consistency and reliability of our findings.

CMIP6

In this study, the most recent climate model, CMIP6, agrees with the earlier versions of the model, i.e., CMIP5, in predicting an increase in precipitation for the Town of Willoughby in the future, in contrast to the TS-1. The findings indicate that even with the lowest SSP scenario (SSP126), there will be an increase in rainfall intensity in TS-2, with a range of

3–19% (Figure 5). Based on the data studied for the Town of Willoughby, it is interesting to note that the magnitude of the increase in the intensity of rainfall varies across different durations and return periods. The two-year return period for a six-hour rainfall shows the lowest percentage increase in intensity. On the other hand, the return period of 100 years for rainfall lasting two hours shows the largest percentage increase in intensity. The projected findings indicate that in the TS-3, the intensity of precipitation is anticipated to undergo a more pronounced increase, where the projected range of increase falls within a range of 7–40% (Figure 6). For a duration of 24 hours and a recurrence interval of two years, a predicted increase in intensity of only 7% is made. However, the two-hour duration with a 100-year return period is predicted to see the highest percentage increase, at 40%. Furthermore, the IDF curve comparison for SSP245 reveals that the TS-2 may experience a rise in precipitation intensity of 5-22% (Figure 7), while the TS-3 could see an increase of 10–23%, as illustrated in Figure 8. This contrast in trends emphasizes the significance of evaluating various time segments when analyzing future climate projections, enabling a deeper understanding of the evolving patterns of precipitation. Likewise, the SSP370 scenario predicts intriguing insights about the future of precipitation intensity. In particular, hourly precipitation with a return period of two years is predicted to increase in intensity, with the lowest observed increase of 5%. The most significant increase in intensity, however, is expected for the two-hour duration of precipitation with a 100-year return period; this is projected to increase by a significant 22%. The comparison of the IDF curves between the TS-1 and the TS-2 for SSP370 is presented in Figure 9, which shows an increase range of 21-38% for various rainfall durations and return periods.

Figure 10 displays the comparison between the TS-1 and the TS-3 for scenario SSP370. In the same manner, the SSP585 scenario under the CMIP6 model demonstrated an increase in precipitation intensity, with a projected range of 9–27% and 21–48% for the TS-2 and TS-3, respectively, for various durations and return periods. The results show that in the most catastrophic scenario (SSP585), hourly precipitation with a 100-year return period will rise by an average of approximately 24% in the future. The IDF curve analysis for the worst-case scenario for CMIP6 is presented in Figure 11, showing the comparison between the TS-1 and the TS-2, whereas the further increase in precipitation in the TS-3 is demonstrated in Figure 12. The increase in precipitation in terms of percentage change considering different return periods and rainfall durations, both for the TS-2 and the TS-3, as compared to the TS-1, is represented in Figure 13. Earlier research by Minallah and Steiner (2021) in the Great Lakes region found that CMIP6 models' representations of precipitation vary widely and contrast with those observed in real-world datasets. Nonetheless, the MIROC6 model used in this study agrees with the similar trend in increased precipitation presented by Minallah & Steiner (2021), indicating the reliability of the findings and validating the predictive ability of the model for future precipitation patterns.

CMIP5 vs. CMIP6: A Comparison

The study revealed that the increase in rainfall intensity for various duration hours and return periods for CMIP5 RCP8.5 and CMIP6 SSP585 is projected to be within the range of 9–39% and 20–55% for the TS-2 and TS-3, respectively. This information has been inferred from Figure 14, which shows the comparison of the TS-2 for both CMIP5 RCP8.5 and CMIP6 SSP585. Similarly, Figure 15 shows the plots of the TS-3 for both CMIPs,

which show that the Town of Willoughby will experience more intense precipitation. The CMIP6 models were assessed under various scenarios, including ssp126, ssp245, ssp370, and ssp585, revealing an increase in precipitation intensity from 2–22% for the TS-2 and 6–40% for the TS-3 across various rainfall durations and return periods. Even though both CMIPs indicate an increase in precipitation intensity, the CMIP5 RCP8.5 stands out with a higher rainfall intensity than the CMIP6 SSP585, with an intensity range that exceeds the CMIP6 SSP585 by 28% across varying durations and return periods.

The findings from the CMIP5 and CMIP6 models provide a fascinating revelation when looking at the percentage increase in rainfall intensity across different durations and return periods. CMIP5 predicts a more substantial increase in rainfall intensity for longer durations and higher return periods, while CMIP6 offers a contrast. There is a clear upward trend in intensity percentage for shorter durations (one and two hours), but an intriguing deviation from this pattern for longer durations (six, twelve, and twenty-four hours).

During the analysis of meteorological data in this study, it was observed that the sub-daily intensity of precipitation, specifically those below 6 hours, was relatively underestimated by the models. Both CMIP5 and CMIP6 models tend to predict less even in the worst-case scenario. This finding is significant because it affects the precision and reliability of outcomes. There was a discrepancy between the study's findings and the historical data reported by the National Oceanic and Atmospheric Administration (NOAA). One possible explanation for the discrepancies found in the data is that lakes were either simplified or left out entirely from the climate models used to examine potential future climate changes. The credibility of the CMIP5 models' projections was called into question by a previous study by Briley et al. (2021), which found that most of them did not accurately capture the

impact of the Great Lakes on the regional climate. Inaccurately simulating regional climate patterns requires a thorough understanding of the interaction between lakes, the atmosphere, and the land. This highlights the need for additional research on the accuracy of sub-daily data and casts doubt on the applicability of the models used.

The study in the town of Willoughby found that the intensity of precipitation would increase with longer return periods. The hourly precipitation is expected to see an increase in the upper range of extreme values in the future, specifically for the 95th percentile. This means that the most severe precipitation events that happen only 5% of the time are likely to become more intense, with a projected increase in the 95th percentile range of 5% to 24%, and the average hourly rainfall in the TS-2 and TS-3 is expected to increase by 7–28% by both CMIPs, which is a signal that communities need to prepare for the impacts of extreme weather events and invest in measures to build more resilient communities in the face of a changing climate. The results show that extreme weather events will become more intense, requiring sustainable development to mitigate urban flooding.

However, it is essential to acknowledge the limitations of this study, such as the fact that it is based on the rainfall estimates of a single location and may not be representative of other areas. Further studies could be accomplished to explore the limitations and make improvements, such as potential uncertainties in the models, data, and bias correction methods used. Regardless, the results of this study provide valuable insights for urban planners, engineers, and decision-makers in developing sustainable flood control measures to mitigate the limitations. Additionally, there's a chance that the study's bias correction methods, data, and models will all have uncertainties that will affect the results. Further studies may explore these limitations and improve upon them.

Conclusion

This study aimed to develop and compare the IDF curves for future climate scenarios using two climate models, CMIP5 and CMIP6, in the town of Willoughby and to evaluate the differences between them. IDF curves are used as an essential tool in designing effective drainage systems for any engineering project. To develop the IDF curves, simulated precipitation data from historical and future periods was used. The data was adjusted to reduce biases using the quantile mapping approach, and the bias-corrected climate data was used to develop the IDF curves using the Gumbel Extreme Distribution Type I method. The results indicated a rise in precipitation intensity in the future, ranging from 9–55% across different rainfall durations and return periods for CMIP5 RCP8.5 and CMIP6 SSP585. The analysis of CMIP6 climate scenarios predicts a significant average increase of 27% in the intensity of hourly precipitation for the recurrence interval of 100 years in the future. Specifically, the SSP585 scenario projects an increase of 9–26% in the TS-2 and 21–47% in the TS-3, while the RCP8.5 scenario predicts increases of 11% to 24%, respectively. Even under the moderate climate change scenario of SSP126, it can be expected to have an increase (averaging 6%) in hourly precipitation intensity with a 2-year return period.

The reliance on a limited number of models and scenarios may not account for the entire range of uncertainty in future scenarios. In this context, further research is needed to understand the combined effects of these uncertainties with other sources of variability, such as land use change and natural internal weather variability. The large uncertainty is the output of the GCMs, and the RCMs also highlight the need for uncertainty analysis and probability-based IDF curves. Furthermore, the process of bias correction in a climate

model is not immune to uncertainties. Future forecasts of climatic variables may be subject to uncertainty after being corrected for bias in climate models, even when based on a single reference period. Hence, future climate results may vary depending on the reference period selected. Future research could explore various methods for responding to all these unknowns, such as using the professional analysis of climatologists or utilizing more robust statistical methods or machine learning algorithms. There is a need for a hybrid approach that makes use of many reference periods due to the complex nature of the interrelationships between climatic variables.

To sum up, the study emphasizes the importance of updating the existing IDF curves that guide the design of water management infrastructure to account for the effects of climate change.

References

- Abatzoglou, J. T., & Brown, T. J. (2012). A comparison of statistical downscaling methods suited for wildfire applications. *International Journal of Climatology*, 32(5), 772–780. <https://doi.org/10.1002/joc.2312>
- Abdulrasheed Mohammed, Salisu Dan'Azumi, Abubakar Ahmed Modibbo, & Abbakar Abbas Adamu. (2021). *Development of Rainfall Intensity Duration Frequency (IDF) Curves for Design of Hydraulic Structures in Kano State, Nigeria*.
- Acharya, N., Chattopadhyay, S., Mohanty, U. C., Dash, S. K., & Sahoo, L. N. (2013). On the bias correction of general circulation model output for Indian summer monsoon. *Meteorological Applications*, 20(3), 349–356. <https://doi.org/10.1002/met.1294>
- Al Islam, M., & Hasan, H. (2020). Generation of IDF equation from catchment delineation using GIS. *Civil Engineering Journal (Iran)*, 6(3), 540–547. <https://doi.org/10.28991/cej-2020-03091490>
- AlHassoun, S. A. (2011). Developing an empirical formulae to estimate rainfall intensity in Riyadh region. *Journal of King Saud University - Engineering Sciences*, 23(2), 81–88. <https://doi.org/10.1016/j.jksues.2011.03.003>
- Allen, M. R., & Ingram, W. J. (2002). *insight review articles 224*. www.nature.com/nature
- Ayugi, B., Shilenje, Z. W., Babaousmail, H., Lim Kam Sian, K. T. C., Mumo, R., Dike, V. N., Iyakaremye, V., Chehbouni, A., & Ongoma, V. (2022). Projected changes in meteorological drought over East Africa inferred from bias-adjusted CMIP6 models. *Natural Hazards*, 113(2), 1151–1176. <https://doi.org/10.1007/s11069-022-05341-8>
- Babaousmail, H., Ayugi, B., Rajasekar, A., Zhu, H., Oduro, C., Mumo, R., & Ongoma, V. (2022). Projection of Extreme Temperature Events over the Mediterranean and Sahara Using Bias-Corrected CMIP6 Models. *Atmosphere*, 13(5). <https://doi.org/10.3390/atmos13050741>
- Babaousmail, H., Hou, R., Ayugi, B., Sian, K. T. C. L. K., Ojara, M., Mumo, R., Chehbouni, A., & Ongoma, V. (2022). Future changes in mean and extreme precipitation over the Mediterranean and Sahara regions using bias-corrected CMIP6 models. *International Journal of Climatology*. <https://doi.org/10.1002/joc.7644>

- Barbero, R., Fowler, H. J., Blenkinsop, S., Westra, S., Moron, V., Lewis, E., Chan, S., Lenderink, G., Kendon, E., Guerreiro, S., Li, X. F., Villalobos, R., Ali, H., & Mishra, V. (2019). A synthesis of hourly and daily precipitation extremes in different climatic regions. *Weather and Climate Extremes*, 26. <https://doi.org/10.1016/j.wace.2019.100219>
- Bartels, R. J., Black, A. W., & Keim, B. D. (2020). Trends in precipitation days in the United States. *International Journal of Climatology*, 40(2), 1038–1048. <https://doi.org/10.1002/joc.6254>
- Berg, P., Moseley, C., & Haerter, J. O. (2013). Strong increase in convective precipitation in response to higher temperatures. *Nature Geoscience*, 6(3), 181–185. <https://doi.org/10.1038/ngeo1731>
- Boberg, F., & Christensen, J. H. (2012). Overestimation of Mediterranean summer temperature projections due to model deficiencies. *Nature Climate Change*, 2(6), 433–436. <https://doi.org/10.1038/nclimate1454>
- Briley, L. J., Rood, R. B., & Notaro, M. (2021). Large lakes in climate models: A Great Lakes case study on the usability of CMIP5. *Journal of Great Lakes Research*, 47(2), 405–418. <https://doi.org/10.1016/j.jglr.2021.01.010>
- Bruni, G., Reinoso, R., van de Giesen, N. C., Clemens, F. H. L. R., & ten Veldhuis, J. A. E. (2015). On the sensitivity of urban hydrodynamic modelling to rainfall spatial and temporal resolution. *Hydrology and Earth System Sciences*, 19(2), 691–709. <https://doi.org/10.5194/hess-19-691-2015>
- Bruyère, C. L., Done, J. M., Holland, G. J., & Fredrick, S. (2014). Bias corrections of global models for regional climate simulations of high-impact weather. *Climate Dynamics*, 43(7–8), 1847–1856. <https://doi.org/10.1007/s00382-013-2011-6>
- Chen, H., Sun, J., Lin, W., & Xu, H. (2020). Comparison of CMIP6 and CMIP5 models in simulating climate extremes. In *Science Bulletin* (Vol. 65, Issue 17, pp. 1415–1418). Elsevier B.V. <https://doi.org/10.1016/j.scib.2020.05.015>
- Chen, J., Brissette, F. P., Chaumont, D., & Braun, M. (2013). Finding appropriate bias correction methods in downscaling precipitation for hydrologic impact studies over North America. *Water Resources Research*, 49(7), 4187–4205. <https://doi.org/10.1002/wrcr.20331>

- Cheng, L., & Aghakouchak, A. (2014a). Nonstationary precipitation intensity-duration-frequency curves for infrastructure design in a changing climate. *Scientific Reports*, 4. <https://doi.org/10.1038/srep07093>
- Cheng, L., & Aghakouchak, A. (2014b). Nonstationary precipitation intensity-duration-frequency curves for infrastructure design in a changing climate. *Scientific Reports*, 4. <https://doi.org/10.1038/srep07093>
- Cioffi, F., Lall, U., Rus, E., & Krishnamurthy, C. K. B. (2015). Space-time structure of extreme precipitation in Europe over the last century. *International Journal of Climatology*, 35(8), 1749–1760. <https://doi.org/10.1002/joc.4116>
- Coelho, G. de A., Ferreira, C. M., Johnston, J., Kinter, J. L., Dollan, I. J., & Maggioni, V. (2022). Potential Impacts of Future Extreme Precipitation Changes on Flood Engineering Design Across the Contiguous United States. *Water Resources Research*, 58(4). <https://doi.org/10.1029/2021WR031432>
- Cook, L. M., McGinnis, S., & Samaras, C. (2020a). The effect of modeling choices on updating intensity-duration-frequency curves and stormwater infrastructure designs for climate change. *Climatic Change*, 159(2), 289–308. <https://doi.org/10.1007/s10584-019-02649-6>
- Cook, L. M., McGinnis, S., & Samaras, C. (2020b). The effect of modeling choices on updating intensity-duration-frequency curves and stormwater infrastructure designs for climate change. *Climatic Change*, 159(2), 289–308. <https://doi.org/10.1007/s10584-019-02649-6>
- Cook, L. M., McGinnis, S., & Samaras, C. (2020c). The effect of modeling choices on updating intensity-duration-frequency curves and stormwater infrastructure designs for climate change. *Climatic Change*, 159(2), 289–308. <https://doi.org/10.1007/s10584-019-02649-6>
- Cook, L. M., McGinnis, S., & Samaras, C. (2020d). The effect of modeling choices on updating intensity-duration-frequency curves and stormwater infrastructure designs for climate change. *Climatic Change*, 159(2), 289–308. <https://doi.org/10.1007/s10584-019-02649-6>
- Debbage, N., & Marshall Shepherd, J. (2019). Urban influences on the spatiotemporal characteristics of runoff and precipitation during the 2009 Atlanta flood. *Journal of Hydrometeorology*, 20(1), 3–21. <https://doi.org/10.1175/JHM-D-18-0010.1>

- Degaetano, A. T. (2009). Time-dependent changes in extreme-precipitation return-period amounts in the continental united states. *Journal of Applied Meteorology and Climatology*, 48(10), 2086–2099. <https://doi.org/10.1175/2009JAMC2179.1>
- Donat, M. G., Lowry, A. L., Alexander, L. V., O’Gorman, P. A., & Maher, N. (2016). More extreme precipitation in the world’s dry and wet regions. *Nature Climate Change*, 6(5), 508–513. <https://doi.org/10.1038/nclimate2941>
- Du, Y., Wang, D., Zhu, J., Wang, D., Qi, X., & Cai, J. (2022). Comprehensive assessment of CMIP5 and CMIP6 models in simulating and projecting precipitation over the global land. *International Journal of Climatology*, 42(13), 6859–6875. <https://doi.org/10.1002/joc.7616>
- Easterling, D. R., Meehl, G. A., Parmesan, C., Changnon, S. A., Karl, T. R., & Mearns, L. O. (2000). *Climate Extremes: Observations, Modeling, and Impacts*. <https://www.science.org>
- Elsebaie, I. H. (2012a). Developing rainfall intensity–duration–frequency relationship for two regions in Saudi Arabia. *Journal of King Saud University - Engineering Sciences*, 24(2), 131–140. <https://doi.org/10.1016/j.jksues.2011.06.001>
- Elsebaie, I. H. (2012b). Developing rainfall intensity–duration–frequency relationship for two regions in Saudi Arabia. *Journal of King Saud University - Engineering Sciences*, 24(2), 131–140. <https://doi.org/10.1016/j.jksues.2011.06.001>
- Elsebaie, I. H. (2012c). Developing rainfall intensity–duration–frequency relationship for two regions in Saudi Arabia. *Journal of King Saud University - Engineering Sciences*, 24(2), 131–140. <https://doi.org/10.1016/j.jksues.2011.06.001>
- Endreny, T. A., & Imbeah, N. (2009). Generating robust rainfall intensity-duration-frequency estimates with short-record satellite data. *Journal of Hydrology*, 371(1–4), 182–191. <https://doi.org/10.1016/j.jhydrol.2009.03.027>
- Gershunov, A., & Cayan, D. R. (2003). *Heavy Daily Precipitation Frequency over the Contiguous United States: Sources of Climatic Variability and Seasonal Predictability*.
- Ghasemi Tousi, E., O’Brien, W., Doulabian, S., & Shadmehri Toosi, A. (2021). Climate changes impact on stormwater infrastructure design in Tucson Arizona. *Sustainable Cities and Society*, 72. <https://doi.org/10.1016/j.scs.2021.103014>

- Giorgi, F., Jones, C., & Asrar, G. R. (2009). Addressing climate information needs at the regional level: the CORDEX framework. In *WMO Bulletin* (Vol. 58, Issue 3). <http://wcrp.ipsl>.
- Groisman, P. Y., Knight, R. W., Easterling, D. R., Karl, T. R., Hegerl, G. C., & Razuvaev, V. N. (2005a). *Trends in Intense Precipitation in the Climate Record*.
- Groisman, P. Y., Knight, R. W., Easterling, D. R., Karl, T. R., Hegerl, G. C., & Razuvaev, V. N. (2005b). *Trends in Intense Precipitation in the Climate Record*.
- Groisman, P. Y., Knight, R. W., & Karl, T. R. (2012). Changes in intense precipitation over the Central United States. *Journal of Hydrometeorology*, 13(1), 47–66. <https://doi.org/10.1175/JHM-D-11-039.1>
- Grose, M. R., Post, D. A., Ling, F. L. N., Corney, S., Bennett, J. C., Grose, M. R., Post, D. A., Ling, F. L. N., Corney, S. P., & Bindoff, N. L. (2011). *Performance of quantile-quantile bias-correction for use in hydroclimatological projections Bioregional Assessment Programme View project Barwon Water inflows under climate change View project Performance of quantile-quantile bias-correction for use in hydroclimatological projections*. <http://mssanz.org.au/modsim2011>
- Grum, M., Jørgensen, A. T., Johansen, R. M., & Linde, J. J. (2006). The effect of climate change on urban drainage: an evaluation based on regional climate model simulations. *Water Science and Technology*, 54(6–7), 9–15.
- Gudmundsson, L., Bremnes, J. B., Haugen, J. E., & Engen-Skaugen, T. (2012). Technical Note: Downscaling RCM precipitation to the station scale using statistical transformations – A comparison of methods. *Hydrology and Earth System Sciences*, 16(9), 3383–3390. <https://doi.org/10.5194/hess-16-3383-2012>
- Guo, Y., & Asce, M. (2006a). *Updating Rainfall IDF Relationships to Maintain Urban Drainage Design Standards*. <https://doi.org/10.1061/ASCE1084-0699200611:5506>
- Guo, Y., & Asce, M. (2006b). *Updating Rainfall IDF Relationships to Maintain Urban Drainage Design Standards*. <https://doi.org/10.1061/ASCE1084-0699200611:5506>
- Gupta, R., Bhattarai, R., & Mishra, A. (2019). Development of climate data bias corrector (CDBC) tool and its application over the agro-ecological zones of India. *Water (Switzerland)*, 11(5). <https://doi.org/10.3390/w11051102>
- Gutowski, J. W., Giorgi, F., Timbal, B., Frigon, A., Jacob, D., Kang, H. S., Raghavan, K., Lee, B., Lennard, C., Nikulin, G., O'Rourke, E., Rixen, M., Solman, S., Stephenson, T., & Tangang, F. (2016). WCRP COordinated Regional Downscaling EXperiment

- (CORDEX): A diagnostic MIP for CMIP6. *Geoscientific Model Development*, 9(11), 4087–4095. <https://doi.org/10.5194/gmd-9-4087-2016>
- Gutowski, W. J., Ullrich, P. A., Hall, A., Leung, L. R., O'Brien, T. A., Patricola, C. M., Arritt, R. W., Bukovsky, M. S., Calvin, K. V., Feng, Z., Jones, A. D., Kooperman, G. J., Monier, E., Pritchard, M. S., Pryor, S. C., Qian, Y., Rhoades, A. M., Roberts, A. F., Sakaguchi, K., ... Zarzycki, C. (2021). The ongoing need for high-resolution regional climate models: Process understanding and stakeholder information. *Bulletin of the American Meteorological Society*, 101(5), E664–E683. <https://doi.org/10.1175/BAMS-D-19-0113.1>
- Haddad, K., Rahman, A., & Green, J. (2011). Design rainfall estimation in Australia: A case study using L moments and Generalized Least Squares Regression. *Stochastic Environmental Research and Risk Assessment*, 25(6), 815–825. <https://doi.org/10.1007/s00477-010-0443-7>
- Haerter, J. O., & Berg, P. (2009). Unexpected rise in extreme precipitation caused by a shift in rain type? In *Nature Geoscience* (Vol. 2, Issue 6, pp. 372–373). <https://doi.org/10.1038/ngeo523>
- Hailegeorgis, T. T., Thorolfsson, S. T., & Alfredsen, K. (2013). Regional frequency analysis of extreme precipitation with consideration of uncertainties to update IDF curves for the city of Trondheim. *Journal of Hydrology*, 498, 305–318. <https://doi.org/10.1016/j.jhydrol.2013.06.019>
- Hao, Z., Aghakouchak, A., & Phillips, T. J. (2013). Changes in concurrent monthly precipitation and temperature extremes. *Environmental Research Letters*, 8(3). <https://doi.org/10.1088/1748-9326/8/3/034014>
- Hayhoe, K., Wake, C., Anderson, B., Liang, X. Z., Maurer, E., Zhu, J., Bradbury, J., Degaetano, A., Stoner, A. M., & Wuebbles, D. (2008). Regional climate change projections for the Northeast USA. *Mitigation and Adaptation Strategies for Global Change*, 13(5–6), 425–436. <https://doi.org/10.1007/s11027-007-9133-2>
- He, J., Valeo, C., & Bouchart, F.-C. (2006). Enhancing urban infrastructure investment planning practices for a changing climate. *Water Science and Technology*, 53(10), 13–20.
- Hess, J. J., Malilay, J. N., & Parkinson, A. J. (2008). Climate Change. The Importance of Place. In *American Journal of Preventive Medicine* (Vol. 35, Issue 5, pp. 468–478). <https://doi.org/10.1016/j.amepre.2008.08.024>

- Hosseinzadehtalaei, P., Tabari, H., & Willems, P. (2020). Climate change impact on short-duration extreme precipitation and intensity–duration–frequency curves over Europe. *Journal of Hydrology*, 590. <https://doi.org/10.1016/j.jhydrol.2020.125249>
- Hou, J., Wang, N., Guo, K., Li, D., Jing, H., Wang, T., & Hinkelmann, R. (2020). Effects of the temporal resolution of storm data on numerical simulations of urban flood inundation. *Journal of Hydrology*, 589. <https://doi.org/10.1016/j.jhydrol.2020.125100>
- Huang, Y., Bárdossy, A., & Zhang, K. (2019). Sensitivity of hydrological models to temporal and spatial resolutions of rainfall data. *Hydrology and Earth System Sciences*, 23(6), 2647–2663. <https://doi.org/10.5194/hess-23-2647-2019>
- IPCC. (2007). *Climate Change 2007: Synthesis Report Summary for Policymakers An Assessment of the Intergovernmental Panel on Climate Change*.
- IPCC. (2014). *Climate change 2014 : synthesis report : longer report*.
- ISFRAM 2015. (2016). In *ISFRAM 2015*. Springer Singapore. <https://doi.org/10.1007/978-981-10-0500-8>
- Karl, T. R., & Knight, R. W. (1998). *Secular Trends of Precipitation Amount, Frequency, and Intensity in the United States*.
- Karl, T. R., Knight, R. W., & Plummer, N. (1995). Trends in high-frequency climate variability in the twentieth century. *Nature*, 377(6546), 217–220. <https://doi.org/10.1038/377217a0>
- Kirtman, B., & Pirani, A. (2009). The State of the Art of Seasonal Prediction: Outcomes and Recommendations from the First World Climate Research Program Workshop on Seasonal Prediction. *Source: Bulletin of the American Meteorological Society*, 90(4), 455–458. <https://doi.org/10.2307/26220969>
- Kourtis, I. M., & Tsihrintzis, V. A. (2022a). Update of intensity-duration-frequency (IDF) curves under climate change: a review. *Water Supply*, 22(5), 4951–4974. <https://doi.org/10.2166/ws.2022.152>
- Kourtis, I. M., & Tsihrintzis, V. A. (2022b). Update of intensity-duration-frequency (IDF) curves under climate change: a review. *Water Supply*, 22(5), 4951–4974. <https://doi.org/10.2166/ws.2022.152>

- Kundwa, M. J. (2019). Development of Rainfall Intensity Duration Frequency (IDF) Curves for Hydraulic Design Aspect. *Journal of Ecology & Natural Resources*, 3(2). <https://doi.org/10.23880/jenr-16000162>
- Kunkel, K. E., Karl, T. R., Brooks, H., Kossin, J., Lawrimore, J. H., Arndt, D., Bosart, L., Changnon, D., Cutter, S. L., Doesken, N., Emanuel, K., Groisman, P. Y., Katz, R. W., Knutson, T., O'Brien, J., Paciorek, C. J., Peterson, T. C., Redmond, K., Robinson, D., ... Wuebbles, D. (2013). Monitoring and understanding trends in extreme storms: State of knowledge. *Bulletin of the American Meteorological Society*, 94(4), 499–514. <https://doi.org/10.1175/BAMS-D-11-00262.1>
- Lafon, T., Dadson, S., Buys, G., & Prudhomme, C. (2013). Bias correction of daily precipitation simulated by a regional climate model: A comparison of methods. *International Journal of Climatology*, 33(6), 1367–1381. <https://doi.org/10.1002/joc.3518>
- Lee, J. W., Hong, S. Y., Chang, E. C., Suh, M. S., & Kang, H. S. (2014). Assessment of future climate change over East Asia due to the RCP scenarios downscaled by GRIMs-RMP. *Climate Dynamics*, 42(3–4), 733–747. <https://doi.org/10.1007/s00382-013-1841-6>
- Lenderink, G., & Van Meijgaard, E. (2008). Increase in hourly precipitation extremes beyond expectations from temperature changes. *Nature Geoscience*, 1(8), 511–514. <https://doi.org/10.1038/ngeo262>
- Li, H., Sheffield, J., & Wood, E. F. (2010). Bias correction of monthly precipitation and temperature fields from Intergovernmental Panel on Climate Change AR4 models using equidistant quantile matching. *Journal of Geophysical Research Atmospheres*, 115(10). <https://doi.org/10.1029/2009JD012882>
- Li, Z., Li, X., Wang, Y., & Quiring, S. M. (2019). Impact of climate change on precipitation patterns in Houston, Texas, USA. *Anthropocene*, 25. <https://doi.org/10.1016/j.ancene.2019.100193>
- Lim Kam Sian, K. T. C., Hagan, D. F. T., Ayugi, B. O., Nooni, I. K., Ullah, W., Babaousmail, H., & Ongoma, V. (2022). Projections of precipitation extremes based on bias-corrected Coupled Model Intercomparison Project phase 6 models ensemble over southern Africa. *International Journal of Climatology*. <https://doi.org/10.1002/joc.7707>

- Liu, L. (2023a). The dynamics of early-stage transmission of COVID-19: A novel quantification of the role of global temperature. *Gondwana Research*, 114, 55–68. <https://doi.org/10.1016/j.gr.2021.12.010>
- Liu, L. (2023b). The dynamics of early-stage transmission of COVID-19: A novel quantification of the role of global temperature. *Gondwana Research*, 114, 55–68. <https://doi.org/10.1016/j.gr.2021.12.010>
- Liu, S., Li, Y., Pauwels, V. R. N., & Walker, J. P. (2018). Impact of rain gauge quality control and interpolation on streamflow simulation: An application to the warwick catchment, Australia. *Frontiers in Earth Science*, 5. <https://doi.org/10.3389/feart.2017.00114>
- Lopez-Cantu, T., Prein, A. F., & Samaras, C. (2020). Uncertainties in Future U.S. Extreme Precipitation From Downscaled Climate Projections. *Geophysical Research Letters*, 47(9). <https://doi.org/10.1029/2019GL086797>
- Madsen, H., Arnbjerg-Nielsen, K., & Mikkelsen, P. S. (2009a). Update of regional intensity-duration-frequency curves in Denmark: Tendency towards increased storm intensities. *Atmospheric Research*, 92(3), 343–349. <https://doi.org/10.1016/j.atmosres.2009.01.013>
- Madsen, H., Arnbjerg-Nielsen, K., & Mikkelsen, P. S. (2009b). Update of regional intensity-duration-frequency curves in Denmark: Tendency towards increased storm intensities. *Atmospheric Research*, 92(3), 343–349. <https://doi.org/10.1016/j.atmosres.2009.01.013>
- Madsen, H., Mikkelsen, P. S., Rosbjerg, D., & Harremoës, P. (2002). Regional estimation of rainfall intensity-duration-frequency curves using generalized least squares regression of partial duration series statistics. *Water Resources Research*, 38(11), 21-1-21–11. <https://doi.org/10.1029/2001wr001125>
- Mailhot, A., Duchesne, S., Rivard, G., Nantel, E., Caya, D., & Villeneuve, J. P. (2006). Climate change impacts on the performance of urban drainage systems for southern Québec. *Proceeding of the EIC Climate Change Technology Conference, Ottawa, ON, Canada*, 10.
- Maraun, D. (2016). Bias Correcting Climate Change Simulations - a Critical Review. In *Current Climate Change Reports* (Vol. 2, Issue 4, pp. 211–220). Springer. <https://doi.org/10.1007/s40641-016-0050-x>

- Maraun, D., Shepherd, T. G., Widmann, M., Zappa, G., Walton, D., Gutiérrez, J. M., Hagemann, S., Richter, I., Soares, P. M. M., Hall, A., & Mearns, L. O. (2017). Towards process-informed bias correction of climate change simulations. *Nature Climate Change*, 7(11), 764–773. <https://doi.org/10.1038/nclimate3418>
- Maraun, D., Wetterhall, F., Ireson, A. M., Chandler, R. E., Kendon, E. J., Widmann, M., Brienen, S., Rust, H. W., Sauter, T., Themel, M., Venema, V. K. C., Chun, K. P., Goodess, C. M., Jones, R. G., Onof, C., Vrac, M., & Thiele-Eich, I. (2010). Precipitation downscaling under climate change: Recent developments to bridge the gap between dynamical models and the end user. *Reviews of Geophysics*, 48(3). <https://doi.org/10.1029/2009RG000314>
- Martel, J.-L., Brissette, F. P., Lucas-Picher, P., Troin, M., & Arsenault, R. (2021a). Climate Change and Rainfall Intensity–Duration–Frequency Curves: Overview of Science and Guidelines for Adaptation. *Journal of Hydrologic Engineering*, 26(10). [https://doi.org/10.1061/\(asce\)he.1943-5584.0002122](https://doi.org/10.1061/(asce)he.1943-5584.0002122)
- Martel, J.-L., Brissette, F. P., Lucas-Picher, P., Troin, M., & Arsenault, R. (2021b). Climate Change and Rainfall Intensity–Duration–Frequency Curves: Overview of Science and Guidelines for Adaptation. *Journal of Hydrologic Engineering*, 26(10). [https://doi.org/10.1061/\(asce\)he.1943-5584.0002122](https://doi.org/10.1061/(asce)he.1943-5584.0002122)
- Martel, J.-L., & Mailhot, A. (2018). *Role of Natural Climate Variability in the Detection of Anthropogenic Climate Change Signal for Mean and Extreme Precipitation at Local and Regional Scales*. <https://doi.org/10.1175/JCLI-D-17-0282.s1>
- Maurer, E. P., & Duffy, P. B. (2005). Uncertainty in projections of streamflow changes due to climate change in California. *Geophysical Research Letters*, 32(3), 1–5. <https://doi.org/10.1029/2004GL021462>
- Maurer, E. P., & Pierce, D. W. (2014). Bias correction can modify climate model simulated precipitation changes without adverse effect on the ensemble mean. *Hydrology and Earth System Sciences*, 18(3), 915–925. <https://doi.org/10.5194/hess-18-915-2014>
- McGinnis, S., & Mearns, L. (2021). Building a climate service for North America based on the NA-CORDEX data archive. *Climate Services*, 22. <https://doi.org/10.1016/j.cliser.2021.100233>
- Mehrotra, R., & Sharma, A. (2012). An improved standardization procedure to remove systematic low frequency variability biases in GCM simulations. *Water Resources Research*, 48(12). <https://doi.org/10.1029/2012WR012446>

- Meira, M. A., Freitas, E. S., Coelho, V. H. R., Tomasella, J., Fowler, H. J., Ramos Filho, G. M., Silva, A. L., & Almeida, C. das N. (2022). Quality control procedures for sub-hourly rainfall data: An investigation in different spatio-temporal scales in Brazil. *Journal of Hydrology*, 613. <https://doi.org/10.1016/j.jhydrol.2022.128358>
- Minallah, S., & Steiner, A. L. (2021). *Analysis of the Atmospheric Water Cycle for the Laurentian Great Lakes Region Using CMIP6 Models*. <https://doi.org/10.1175/JCLI-D-20>
- Mirhosseini, G., Srivastava, P., & Stefanova, L. (2013). The impact of climate change on rainfall Intensity-Duration-Frequency (IDF) curves in Alabama. *Regional Environmental Change*, 13(SUPPL.1), 25–33. <https://doi.org/10.1007/s10113-012-0375-5>
- Moraglia, G., Brattich, E., & Carbone, G. (2022). Precipitation trends in North and South Carolina, USA. *Journal of Hydrology: Regional Studies*, 44. <https://doi.org/10.1016/j.ejrh.2022.101201>
- Morrison, A., Villarini, G., Zhang, W., & Scoccimarro, E. (2019). Projected changes in extreme precipitation at sub-daily and daily time scales. *Global and Planetary Change*, 182. <https://doi.org/10.1016/j.gloplacha.2019.103004>
- Mujere, N. (2011). *Flood Frequency Analysis Using the Gumbel Distribution*.
- Noor, M., Ismail, T., Chung, E. S., Shahid, S., & Sung, J. H. (2018). Uncertainty in rainfall intensity duration frequency curves of Peninsular Malaysia under changing climate scenarios. *Water (Switzerland)*, 10(12). <https://doi.org/10.3390/w10121750>
- Noor, M., Ismail, T., Shahid, S., Asaduzzaman, M., & Dewan, A. (2022). Projection of rainfall intensity-duration-frequency curves at ungauged location under climate change scenarios. *Sustainable Cities and Society*, 83. <https://doi.org/10.1016/j.scs.2022.103951>
- Ntegeka, V., & Willems, P. (2008). Trends and multidecadal oscillations in rainfall extremes, based on a more than 100-year time series of 10 min rainfall intensities at Uccle, Belgium. *Water Resources Research*, 44(7). <https://doi.org/10.1029/2007WR006471>
- Obaid, N., Alghazali, S., Adnan, D., & Alawadi, H. (2014). *Fitting Statistical Distributions of Monthly Rainfall for Some Iraqi Stations*. 6(6). www.iiste.org
- O'Neill, B. C., Tebaldi, C., Van Vuuren, D. P., Eyring, V., Friedlingstein, P., Hurtt, G., Knutti, R., Kriegl, E., Lamarque, J. F., Lowe, J., Meehl, G. A., Moss, R., Riahi,

- K., & Sanderson, B. M. (2016). The Scenario Model Intercomparison Project (ScenarioMIP) for CMIP6. *Geoscientific Model Development*, 9(9), 3461–3482. <https://doi.org/10.5194/gmd-9-3461-2016>
- Ouarda, T. B. M. J., Yousef, L. A., & Charron, C. (2019). Non-stationary intensity-duration-frequency curves integrating information concerning teleconnections and climate change. *International Journal of Climatology*, 39(4), 2306–2323. <https://doi.org/10.1002/joc.5953>
- Papa, F., Guo, Y., & Thoman, G. W. (2004). Urban drainage infrastructure planning and management with a changing climate. *Proceedings of the 57th Canadian Water Resources Association Annual Congress—Water and Climate Change: Knowledge for Better Adaptation, Montréal, QC, Canada*, 16–18.
- Park, J. H., Oh, S. G., & Suh, M. S. (2013). Impacts of boundary conditions on the precipitation simulation of RegCM4 in the CORDEX East Asia domain. *Journal of Geophysical Research Atmospheres*, 118(4), 1652–1667. <https://doi.org/10.1002/jgrd.50159>
- Peck, A., Prodanovic, P., & Simonovic, S. P. (2012a). Rainfall intensity duration frequency curves under climate change: City of London, Ontario, Canada. *Canadian Water Resources Journal*, 37(3), 177–189. <https://doi.org/10.4296/cwrj2011-935>
- Peck, A., Prodanovic, P., & Simonovic, S. P. (2012b). Rainfall intensity duration frequency curves under climate change: City of London, Ontario, Canada. *Canadian Water Resources Journal*, 37(3), 177–189. <https://doi.org/10.4296/cwrj2011-935>
- Pierce, D. W., Cayan, D. R., & Thrasher, B. L. (2014). *Statistical Downscaling Using Localized Constructed Analogs (LOCA)**. <https://doi.org/10.1175/JHM-D-14>
- Prein, A. F., Rasmussen, R. M., Ikeda, K., Liu, C., Clark, M. P., & Holland, G. J. (2017). The future intensification of hourly precipitation extremes. *Nature Climate Change*, 7(1), 48–52. <https://doi.org/10.1038/nclimate3168>
- Prodanovic, P., & Simonovic, S. P. (2007). *THE UNIVERSITY OF WESTERN ONTARIO DEPARTMENT OF CIVIL AND ENVIRONMENTAL ENGINEERING Water Resources Research Report*.
- Pui, A., Sharma, A., Mehrotra, R., Sivakumar, B., & Jeremiah, E. (2012). A comparison of alternatives for daily to sub-daily rainfall disaggregation. *Journal of Hydrology*, 470–471, 138–157. <https://doi.org/10.1016/j.jhydrol.2012.08.041>

- Qian, Y., Ghan, S. J., & Leung, L. R. (2010). Downscaling hydroclimatic changes over the western US based on CAM subgrid scheme and WRF regional climate simulations. *International Journal of Climatology*, *30*(5), 675–693. <https://doi.org/10.1002/joc.1928>
- Ragno, E., AghaKouchak, A., Love, C. A., Cheng, L., Vahedifard, F., & Lima, C. H. R. (2018). Quantifying Changes in Future Intensity-Duration-Frequency Curves Using Multimodel Ensemble Simulations. *Water Resources Research*, *54*(3), 1751–1764. <https://doi.org/10.1002/2017WR021975>
- Rashid, M., Faruque, S., Rashid, M. M., Faruque, S. B., & Alam, J. B. (2012). *Modeling of Short Duration Rainfall Intensity Duration Frequency (SDR-IDF) Equation for Sylhet City in Bangladesh Statistical Downscaling of GCM Outputs to Rainfall View project Extreme sea level variations along the U.S. coastlines View project Modeling of Short Duration Rainfall Intensity Duration Frequency (SDR-IDF) Equation for Sylhet City in Bangladesh*. 2(2). <http://www.ejournalofscience.org>
- Rodríguez, R., Navarro, X., Casas, M. C., Ribalaygua, J., Russo, B., Pouget, L., & Redaño, A. (2014). Influence of climate change on IDF curves for the metropolitan area of Barcelona (Spain). *International Journal of Climatology*, *34*(3), 643–654. <https://doi.org/10.1002/joc.3712>
- Rummukainen, M. (2016). Added value in regional climate modeling. *Wiley Interdisciplinary Reviews: Climate Change*, *7*(1), 145–159. <https://doi.org/10.1002/wcc.378>
- Shrestha, A., Babel, M. S., Weesakul, S., & Vojinovic, Z. (2017). Developing Intensity-Duration-Frequency (IDF) curves under climate change uncertainty: The case of Bangkok, Thailand. *Water (Switzerland)*, *9*(2). <https://doi.org/10.3390/w9020145>
- Shrestha, S., Sharma, S., Gupta, R., & Bhattarai, R. (2019). Impact of global climate change on stream low flows: A case study of the great Miami river Watershed, Ohio. *International Journal of Agricultural and Biological Engineering*, *12*(1), 84–95. <https://doi.org/10.25165/j.ijabe.20191201.4486>
- Singh, R., Arya, D. S., Taxak, A. K., & Vojinovic, Z. (2016). Potential Impact of Climate Change on Rainfall Intensity-Duration-Frequency Curves in Roorkee, India. *Water Resources Management*, *30*(13), 4603–4616. <https://doi.org/10.1007/s11269-016-1441-4>
- Sohoulande Djebou, C. D., Conger, S., Szogi, A. A., Stone, K. C., & Martin, J. H. (2021). Seasonal precipitation pattern analysis for decision support of agricultural irrigation

- management in Louisiana, USA. *Agricultural Water Management*, 254. <https://doi.org/10.1016/j.agwat.2021.106970>
- Solomon, O., & Prince, O. (2013). *Flood Frequency Analysis of Osse River Using Gumbel's Distribution*. 3(10). www.iiste.org
- Sowby, R. B., & Capener, A. (2023). The influence of precipitation on the energy footprint of Denver's water supply: A 20-year analysis and implications for climate change. *Energy Nexus*, 9, 100166. <https://doi.org/10.1016/j.nexus.2022.100166>
- Srivastav, R. K., Schardong, A., & Simonovic, S. P. (2014). Equidistance Quantile Matching Method for Updating IDF Curves under Climate Change. *Water Resources Management*, 28(9), 2539–2562. <https://doi.org/10.1007/s11269-014-0626-y>
- Statkewicz, M. D., Talbot, R., & Rappenglueck, B. (2021). Changes in precipitation patterns in Houston, Texas. *Environmental Advances*, 5. <https://doi.org/10.1016/j.envadv.2021.100073>
- Sun, X., Thyer, M., Renard, B., & Lang, M. (2014). A general regional frequency analysis framework for quantifying local-scale climate effects: A case study of ENSO effects on Southeast Queensland rainfall. *Journal of Hydrology*, 512, 53–68. <https://doi.org/10.1016/j.jhydrol.2014.02.025>
- Sunyer, M. A., Madsen, H., Rosbjerg, D., & Arnbjerg-Nielsen, K. (2014). A Bayesian approach for uncertainty quantification of extreme precipitation projections including climate model interdependency and nonstationary bias. *Journal of Climate*, 27(18), 7113–7132. <https://doi.org/10.1175/JCLI-D-13-00589.1>
- Swain, D. L., Wing, O. E. J., Bates, P. D., Done, J. M., Johnson, K. A., & Cameron, D. R. (2020). Increased Flood Exposure Due to Climate Change and Population Growth in the United States. *Earth's Future*, 8(11). <https://doi.org/10.1029/2020EF001778>
- Tabari, H. (2020). Climate change impact on flood and extreme precipitation increases with water availability. *Scientific Reports*, 10(1). <https://doi.org/10.1038/s41598-020-70816-2>
- Tabari, H., Paz, S. M., Buekenhout, D., & Willems, P. (2021). Comparison of statistical downscaling methods for climate change impact analysis on precipitation-driven drought. *Hydrology and Earth System Sciences*, 25(6), 3493–3517. <https://doi.org/10.5194/hess-25-3493-2021>

- Thakali, R., Kalra, A., & Ahmad, S. (2016). Understanding the effects of climate change on urban stormwater infrastructures in the Las Vegas Valley. *Hydrology*, 3(4). <https://doi.org/10.3390/hydrology3040034>
- Thibeault, J. M., & Seth, A. (2014). Changing climate extremes in the Northeast United States: observations and projections from CMIP5. *Climatic Change*, 127(2), 273–287. <https://doi.org/10.1007/s10584-014-1257-2>
- Thomas R. Karl, Jerry M. Melillo, & Thomas C. Peterson. (2009). *Global Climate Change Impacts in the United States: a state of knowledge report from the U.S. Global Change Research Program*. <http://hdl.handle.net/1834/20072>
- Tiwari, S., Jha, S. K., & Singh, A. (2020). Quantification of node importance in rain gauge network: influence of temporal resolution and rain gauge density. *Scientific Reports*, 10(1). <https://doi.org/10.1038/s41598-020-66363-5>
- Trenberth, K. E. (2011). Changes in precipitation with climate change. *Climate Research*, 47(1–2), 123–138. <https://doi.org/10.3354/cr00953>
- Trenberth, K. E., Dai, A., Rasmussen, R. M., & Parsons, D. B. (2003). *THE CHANGING CHARACTER OF PRECIPITATION*.
- Trenberth, K. E., & Zhang, Y. (2018). Near-global covariability of hourly precipitation in space and time. *Journal of Hydrometeorology*, 19(4), 695–713. <https://doi.org/10.1175/JHM-D-17-0238.1>
- Vidal, I. (2014). A Bayesian analysis of the Gumbel distribution: An application to extreme rainfall data. *Stochastic Environmental Research and Risk Assessment*, 28(3), 571–582. <https://doi.org/10.1007/s00477-013-0773-3>
- Weathers, M., Hathaway, J. M., Tirpak, R. A., & Khojandi, A. (2023). Evaluating the impact of climate change on future bioretention performance across the contiguous United States. *Journal of Hydrology*, 616. <https://doi.org/10.1016/j.jhydrol.2022.128771>
- Weldegerima, T. M., Zeleke, T. T., Birhanu, B. S., Zaitchik, B. F., & Fetene, Z. A. (2018). Analysis of Rainfall Trends and Its Relationship with SST Signals in the Lake Tana Basin, Ethiopia. *Advances in Meteorology*, 2018. <https://doi.org/10.1155/2018/5869010>
- Westra, S., Fowler, H. J., Evans, J. P., Alexander, L. V., Berg, P., Johnson, F., Kendon, E. J., Lenderink, G., & Roberts, N. M. (2014). Future changes to the intensity and frequency of short-duration extreme rainfall. In *Reviews of Geophysics* (Vol. 52,

Issue 3, pp. 522–555). Blackwell Publishing Ltd.
<https://doi.org/10.1002/2014RG000464>

- Westra, S., Renard, B., & Thyer, M. (2015). The ENSO-precipitation teleconnection and its modulation by the interdecadal pacific oscillation. *Journal of Climate*, 28(12), 4753–4773. <https://doi.org/10.1175/JCLI-D-14-00722.1>
- Willems, P. (2013a). Adjustment of extreme rainfall statistics accounting for multidecadal climate oscillations. *Journal of Hydrology*, 490, 126–133. <https://doi.org/10.1016/j.jhydrol.2013.03.034>
- Willems, P. (2013b). Revision of urban drainage design rules after assessment of climate change impacts on precipitation extremes at Uccle, Belgium. *Journal of Hydrology*, 496, 166–177. <https://doi.org/10.1016/j.jhydrol.2013.05.037>
- Wood, A. W., Leung, L. R., Sridhar, V., & Lettenmaier, D. P. (2004a). *HYDROLOGIC IMPLICATIONS OF DYNAMICAL AND STATISTICAL APPROACHES TO DOWNSCALING CLIMATE MODEL OUTPUTS*.
- Wood, A. W., Leung, L. R., Sridhar, V., & Lettenmaier, D. P. (2004b). *HYDROLOGIC IMPLICATIONS OF DYNAMICAL AND STATISTICAL APPROACHES TO DOWNSCALING CLIMATE MODEL OUTPUTS*.
- Xu, Z., & Yang, Z. L. (2012). An improved dynamical downscaling method with GCM bias corrections and its validation with 30 years of climate simulations. *Journal of Climate*, 25(18), 6271–6286. <https://doi.org/10.1175/JCLI-D-12-00005.1>
- Xue, P., Ye, X., Pal, J. S., Chu, P. Y., Kayastha, M. B., & Huang, C. (2022). Climate projections over the Great Lakes Region: using two-way coupling of a regional climate model with a 3-D lake model. *Geoscientific Model Development*, 15(11), 4425–4446. <https://doi.org/10.5194/gmd-15-4425-2022>
- Xue-Jie, G., Mei-Li, W., & Giorgi, F. (2013). Climate Change over China in the 21st Century as Simulated by BCC_CSM1.1-RegCM4.0. *Atmospheric and Oceanic Science Letters*, 6(5), 381–386. <https://doi.org/10.3878/j.issn.1674-2834.13.0029>
- Yan, H., Sun, N., Wigmosta, M., Skaggs, R., Hou, Z., & Leung, L. R. (2019). Next-Generation Intensity–Duration–Frequency Curves to Reduce Errors in Peak Flood Design. *Journal of Hydrologic Engineering*, 24(7). [https://doi.org/10.1061/\(asce\)he.1943-5584.0001799](https://doi.org/10.1061/(asce)he.1943-5584.0001799)
- Yilmaz, A. G., & Perera, B. J. C. (2014). Extreme Rainfall Nonstationarity Investigation and Intensity–Frequency–Duration Relationship. *Journal of Hydrologic*

Engineering, 19(6), 1160–1172. [https://doi.org/10.1061/\(asce\)he.1943-5584.0000878](https://doi.org/10.1061/(asce)he.1943-5584.0000878)

Yong, S. L. S., Ng, J. L., Huang, Y. F., & Ang, C. K. (2021). ASSESSMENT OF THE BEST PROBABILITY DISTRIBUTION METHOD IN RAINFALL FREQUENCY ANALYSIS FOR A TROPICAL REGION. *Malaysian Journal of Civil Engineering*, 33(1). <https://doi.org/10.11113/mjce.v33.16253>

Zhai, P., Zhang, X., & Wan, H. (2005). *Trends in Total Precipitation and Frequency of Daily Precipitation Extremes over China*.

Zhang, L., Zhao, Y., Hein-Griggs, D., Janes, T., Tucker, S., & Ciborowski, J. J. H. (2020). Climate change projections of temperature and precipitation for the great lakes basin using the PRECIS regional climate model. *Journal of Great Lakes Research*, 46(2), 255–266. <https://doi.org/10.1016/j.jglr.2020.01.013>

Zhang, N., Li, Z., Zou, X., & Quiring, S. M. (2019). Comparison of three short-term load forecast models in Southern California. *Energy*, 189. <https://doi.org/10.1016/j.energy.2019.116358>

Zhang, R., & Delworth, T. L. (2006). Impact of Atlantic multidecadal oscillations on India/Sahel rainfall and Atlantic hurricanes. *Geophysical Research Letters*, 33(17). <https://doi.org/10.1029/2006GL026267>

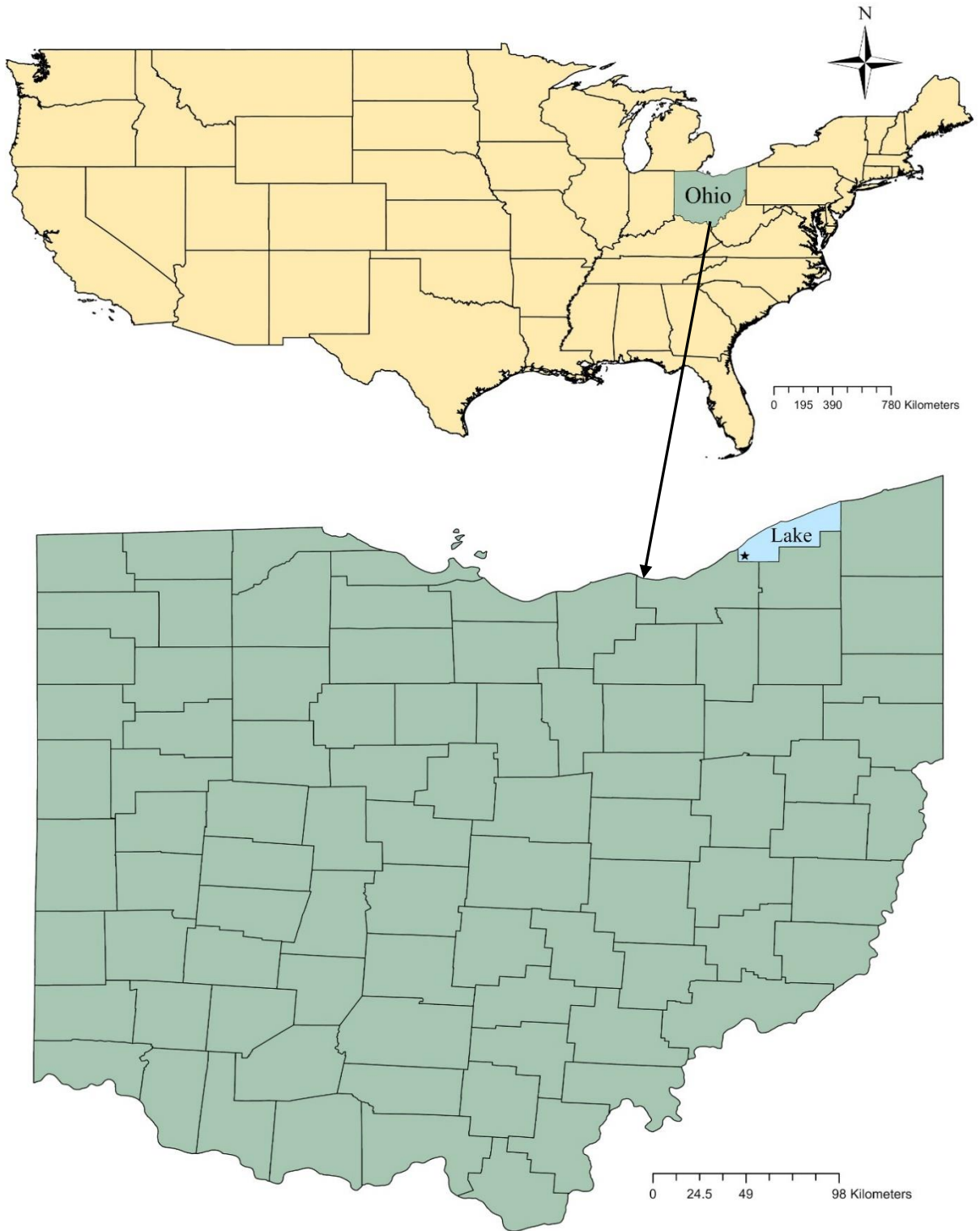
Table 1. Description of the climate models and climate change scenarios used in the study.

CMIP5						
Source	Source ID	GCM	Scenario	Grid	Frequency	Resolution
NA-CORDEX	WRF	GFDL-ESM2M	hist, RCP8.5	NAM-22	1 hr	0.44° x 0.44°
		HadGEM2-ES				
		MPI-ESM-LR				
CMIP6						
Source	Source ID	Experiment ID	Variant Label	Frequency	Resolution	
WRCP	MIROC6	hist, ssp126, ssp245, ssp370, ssp585	r1i1p1f1	1 hr	1.4° x 1.4°	
	CNRM-CM6-1-HR		r1i1p1f2		0.5° x 0.5°	
	CNRM-ESM2-1		r1i1p1f2		1.4° x 1.4°	

Table 2. Bias in terms of mean and standard deviation (St. Dev.) before and after bias correction for CMIP5 and CMIP6 models for the baseline period (TS-1: 1980-2019)

CMIP5 Models							
Statistics	Observed	GFDL-ESM2M		HadGEM2-ES		MPI-ESM-LR	
		Before	After	Before	After	Before	After
Average	2.67	4.04	2.6	3.06	2.68	3.56	2.51
St. Dev.	6.62	7.24	6.78	7.11	6.58	6.79	6.39

CMIP6 Models							
Statistics	Observed	GFDL-ESM2M		HadGEM2-ES		MPI-ESM-LR	
		Before	After	Before	After	Before	After
Average	2.67	3.04	2.69	3.36	2.65	3.30	2.68
St. Dev.	6.62	6.06	6.77	6.60	6.71	6.13	6.77



★ on the map indicates the approximate location of the Town of Willoughby

Figure 1. Location map of the study area showing Town of Willoughby, Ohio, USA

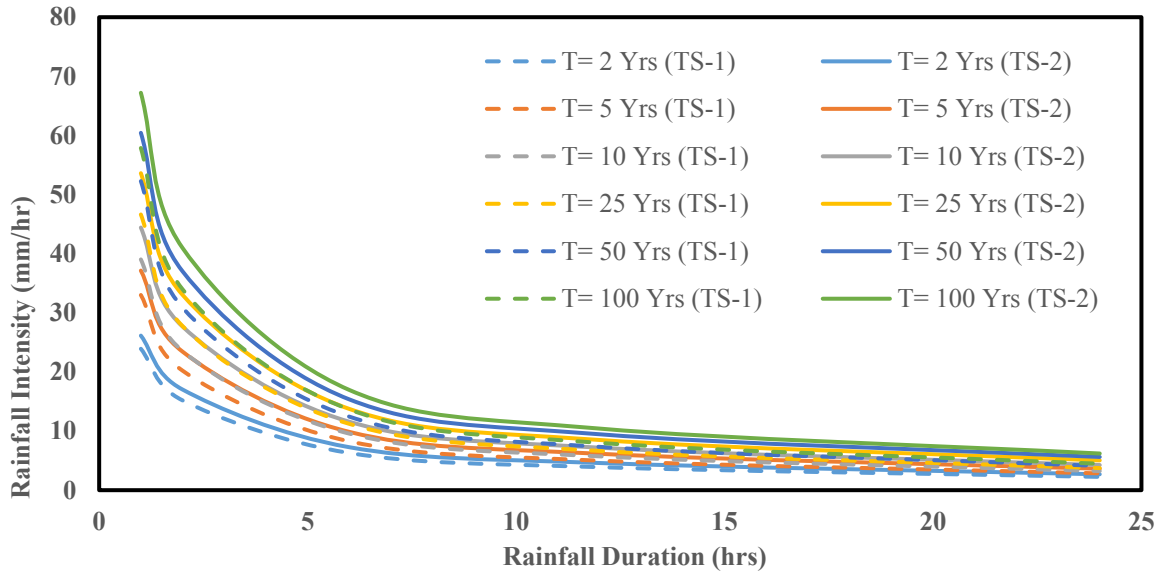


Figure 2. IDF curves for the baseline period (TS-1: 1980-2019) vs. the near future (TS-2: 2020-2059) considering a 2, 5, 10, 25, 50, and 100-year return period ensembling three CMIP5 RCP8.5 models

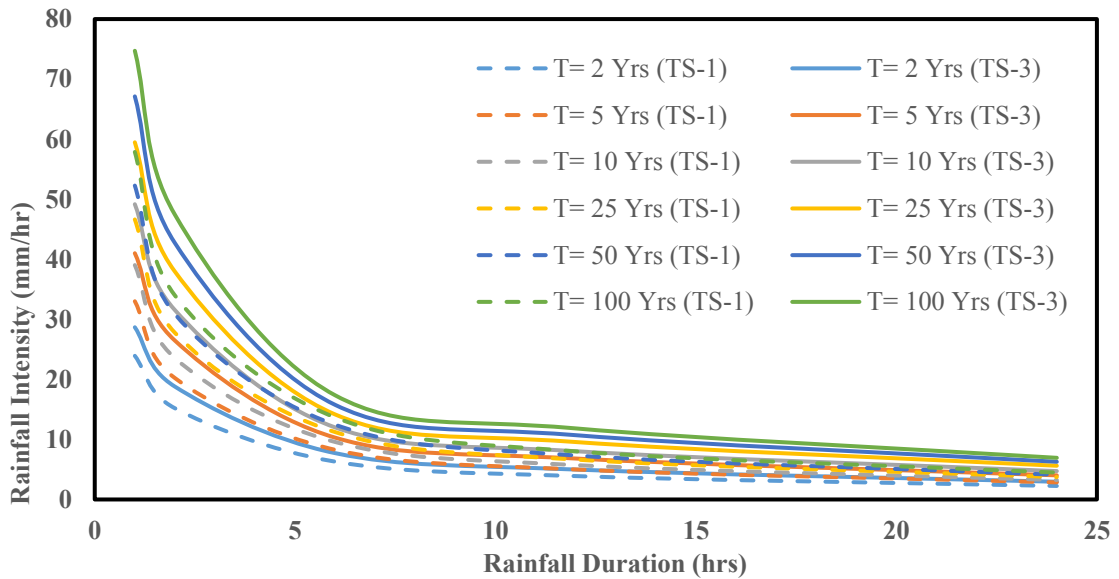


Figure 3. IDF curves for the baseline period (TS-1: 1980–2019) vs. the far future (TS-3: 2060–2099) considering a 2, 5, 10, 25, 50, and 100-year return period ensembling three CMIP5 RCP8.5 models

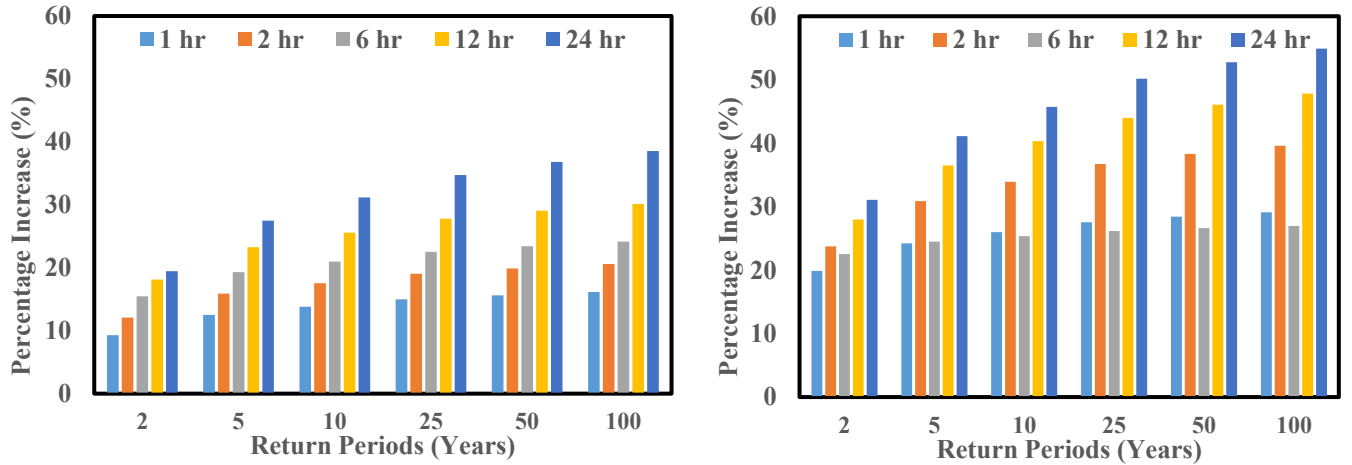


Figure 4. Graphical comparison showing the rainfall intensity percentage change between the baseline period (TS-1: 1980–2019) vs. the near future (TS-2: 2020–2059), on the left, and the baseline period (TS-1: 1980–2019) vs. the far future (TS-3: 2060–2099), on the right, for different return periods and rainfall durations of CMIP5 RCP8.5

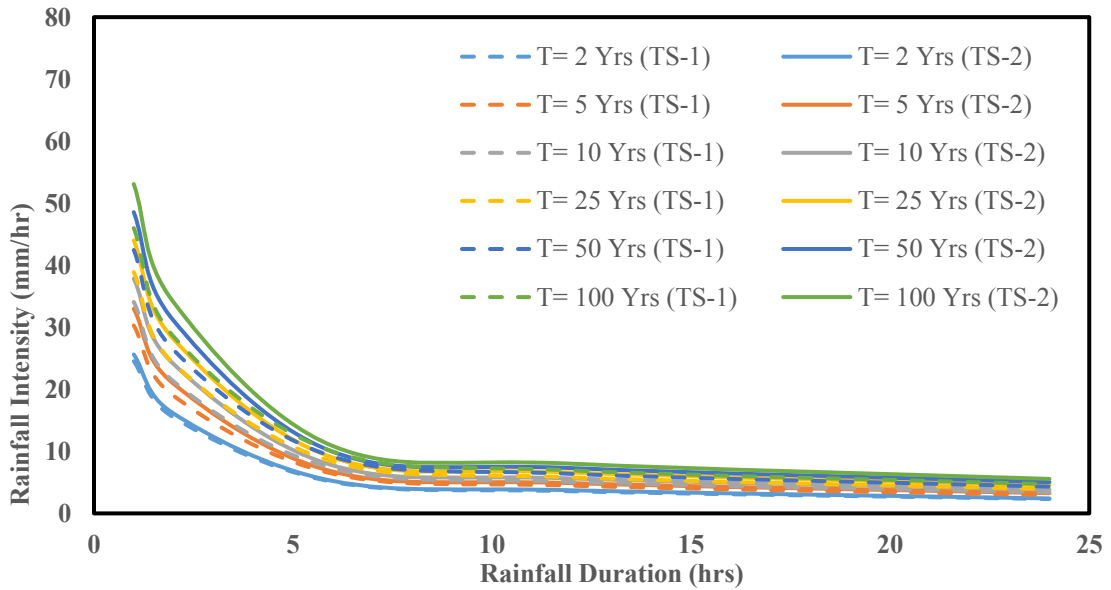


Figure 5. IDF curves for the baseline period (TS-1: 1980–2019) vs. the near future (TS-2: 2020–2059) considering a 2, 5, 10, 25, 50, and 100-year return period ensembling three CMIP6 SSP126 models

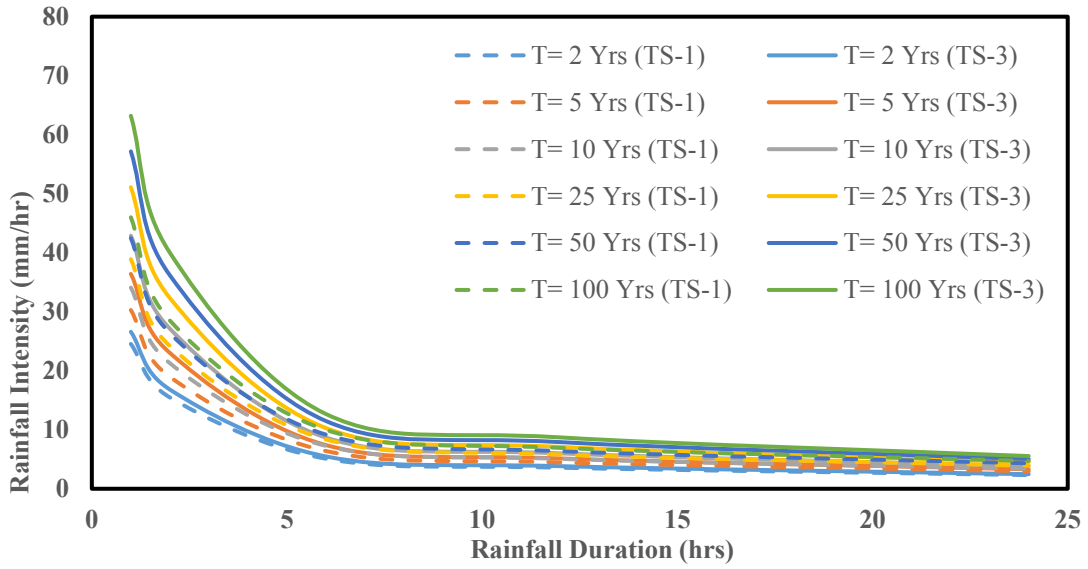


Figure 6. IDF curves for the baseline period (TS-1: 1980–2019) vs. the far future (TS-3: 2060–2099) considering a 2, 5, 10, 25, 50, and 100-year return period ensembling three CMIP6 SSP126 models

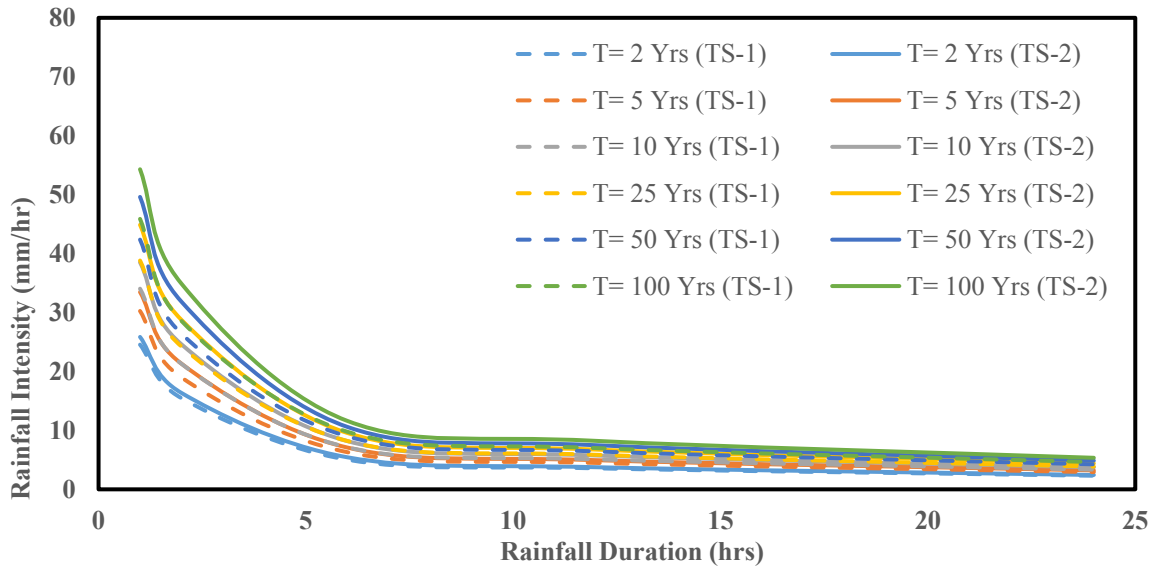


Figure 7. IDF curves for the baseline period (TS-1: 1980–2019) vs. the near future (TS-2: 2020–2059) considering a 2, 5, 10, 25, 50, and 100-year return period ensembling three CMIP6 SSP245 models

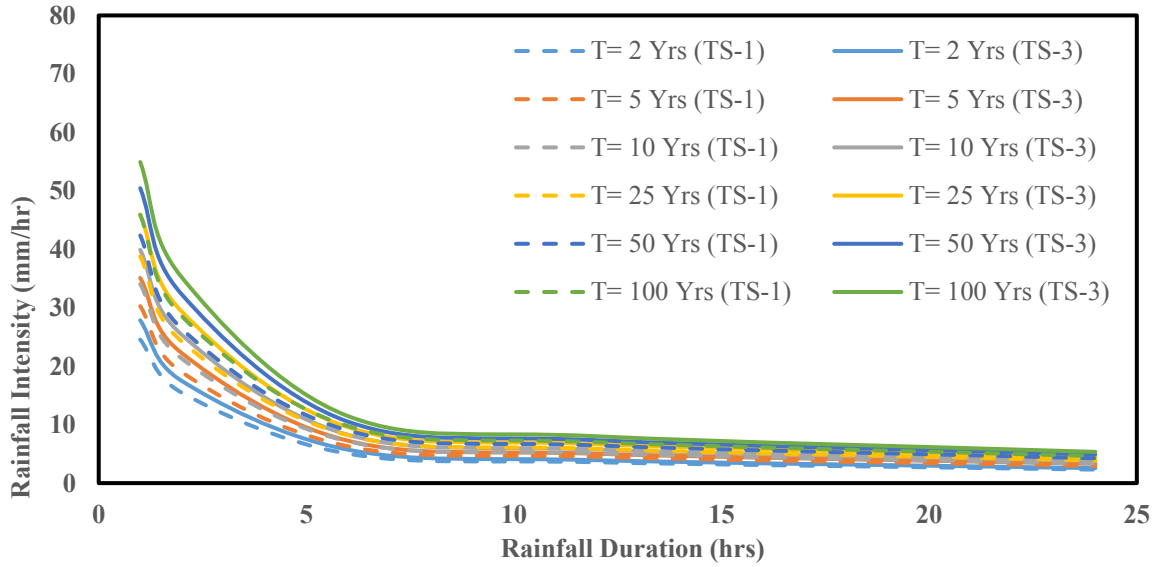


Figure 8. IDF curves for the baseline period (TS-1: 1980–2019) vs. the far future (TS-3: 2060–2099) considering a 2, 5, 10, 25, 50, and 100-year return period ensembling three CMIP6 SSP245 models

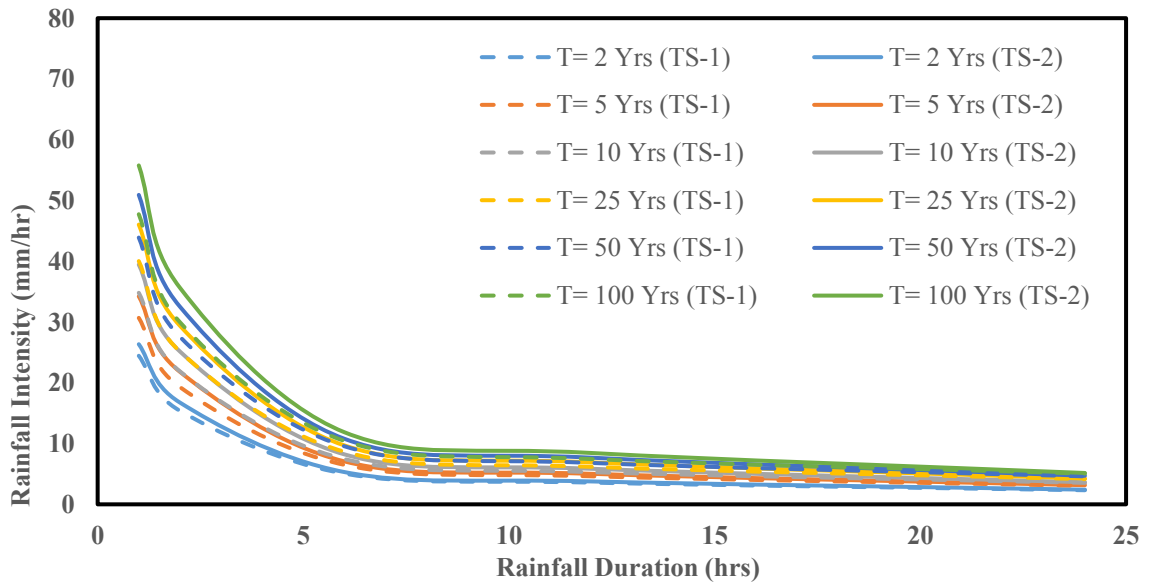


Figure 9. IDF curves for the baseline period (TS-1: 1980–2019) vs. the near future (TS-2: 2020–2059) considering a 2, 5, 10, 25, 50, and 100-year return period ensembling three CMIP6 SSP370 models

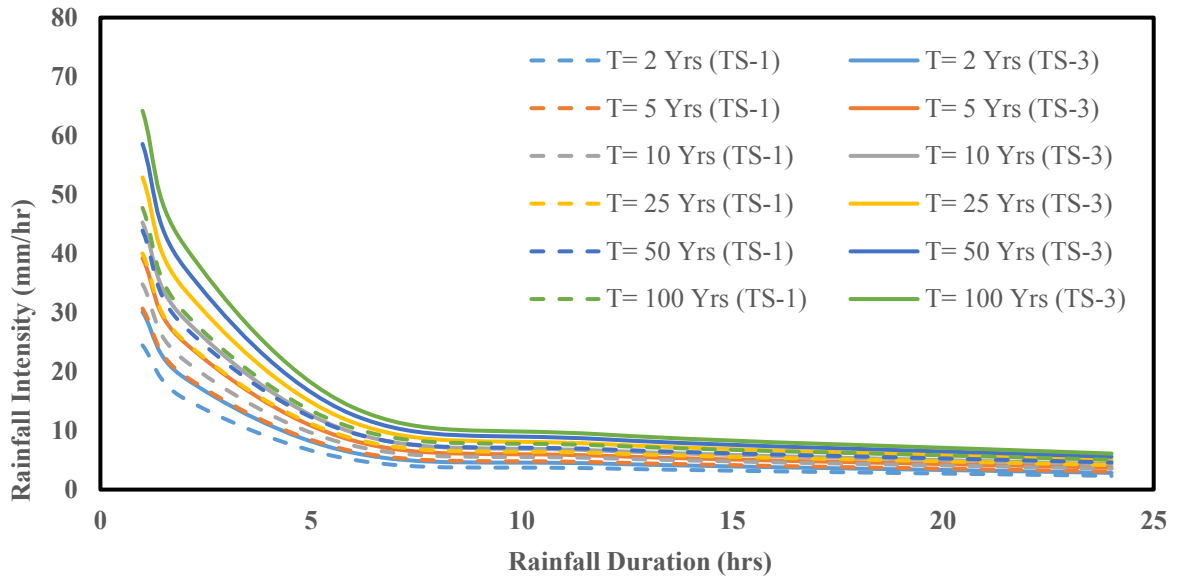


Figure 10. IDF curves for the baseline period (TS-1: 1980–2019) vs. the far future (TS-3: 2060–2099) considering a 2, 5, 10, 25, 50, and 100-year return period ensembling three CMIP6 SSP370 models

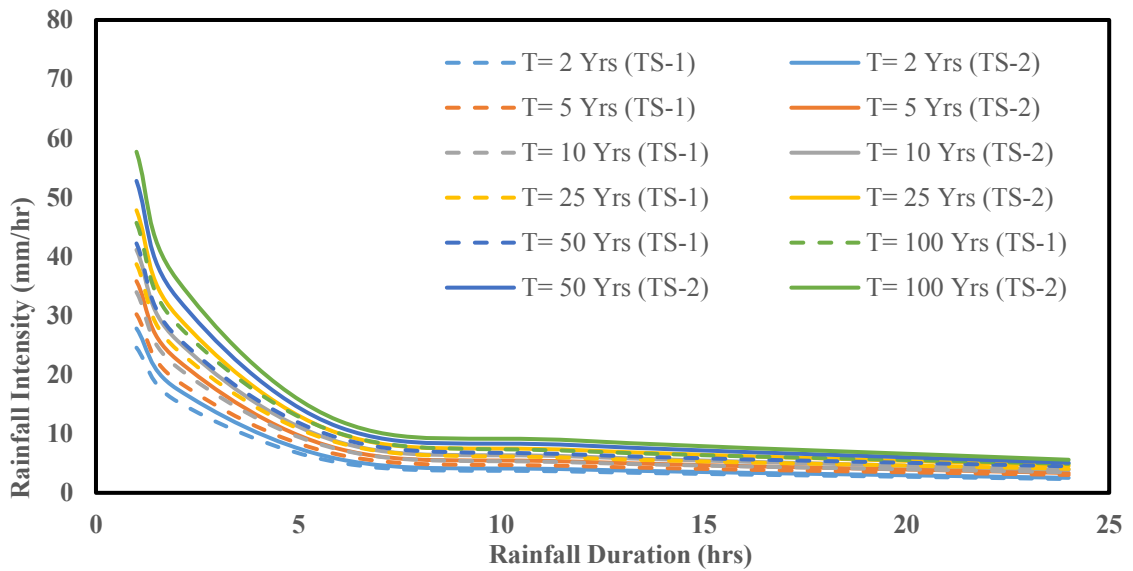


Figure 11. IDF curves for the baseline period (TS-1: 1980–2019) vs. the near future (TS-2: 2020–2059) considering a 2, 5, 10, 25, 50, and 100-year return period ensembling three CMIP6 SSP585 models

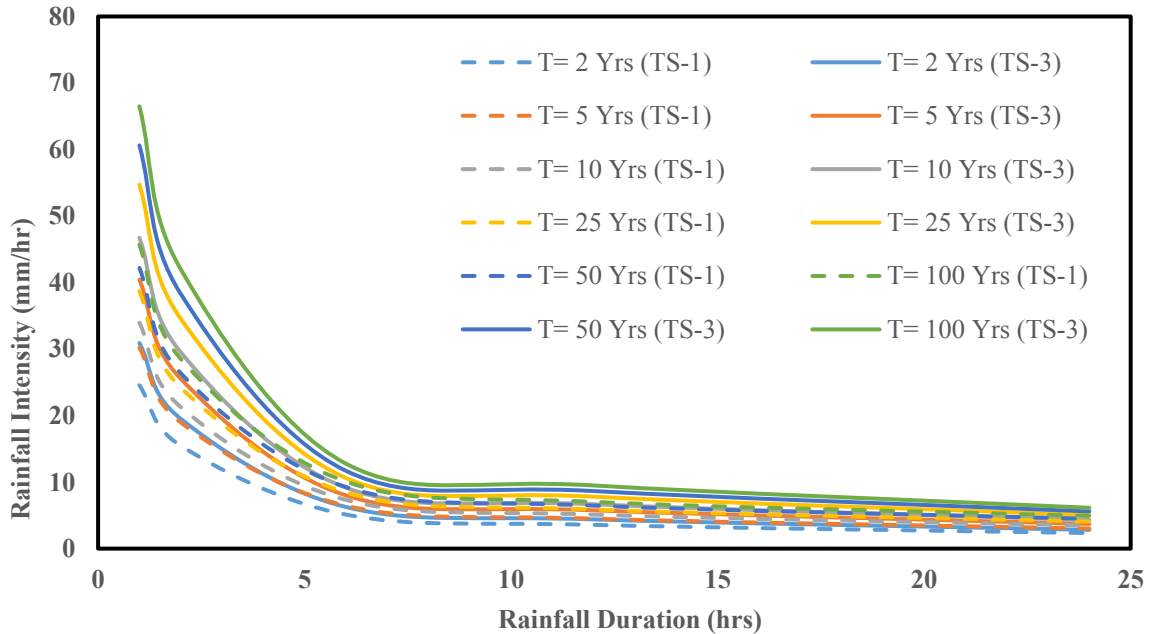


Figure 12. IDF curves for the baseline period (TS-1: 1980–2019) vs. the far future (TS-3: 2060–2099) considering a 2, 5, 10, 25, 50, and 100-year return period ensembling three CMIP6 SSP585 models

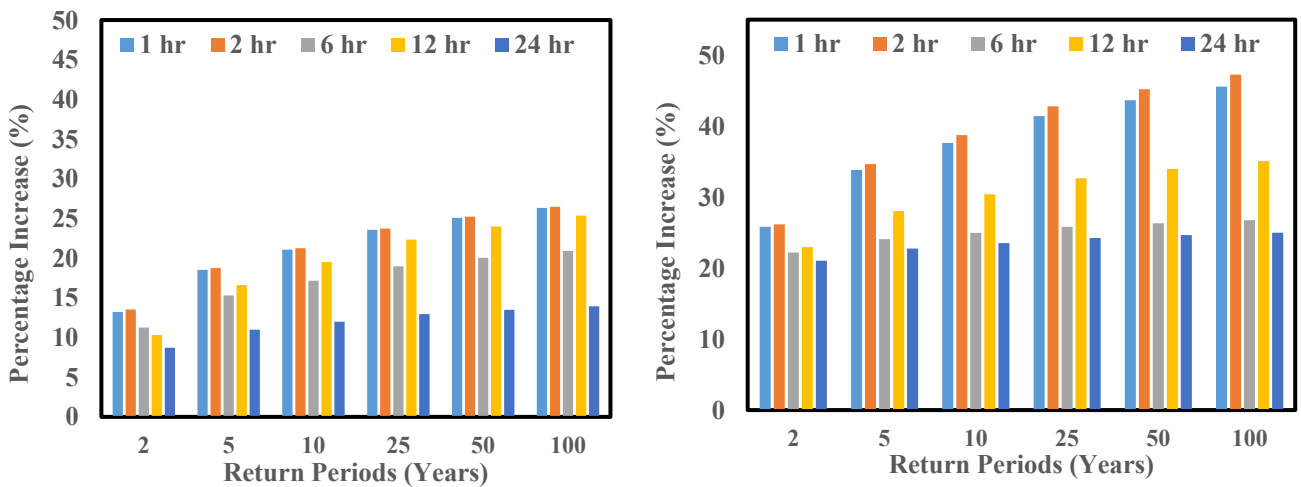


Figure 13. Graphical comparison showing the rainfall intensity percentage change between the baseline period (TS-1: 1980–2019) vs. the near future (TS-2: 2020–2059), on the left, and the baseline period (TS-1: 1980–2019) vs. the far future (TS-3: 2060–2099), on the right, for different return periods and rainfall duration of CMIP6 SSP585

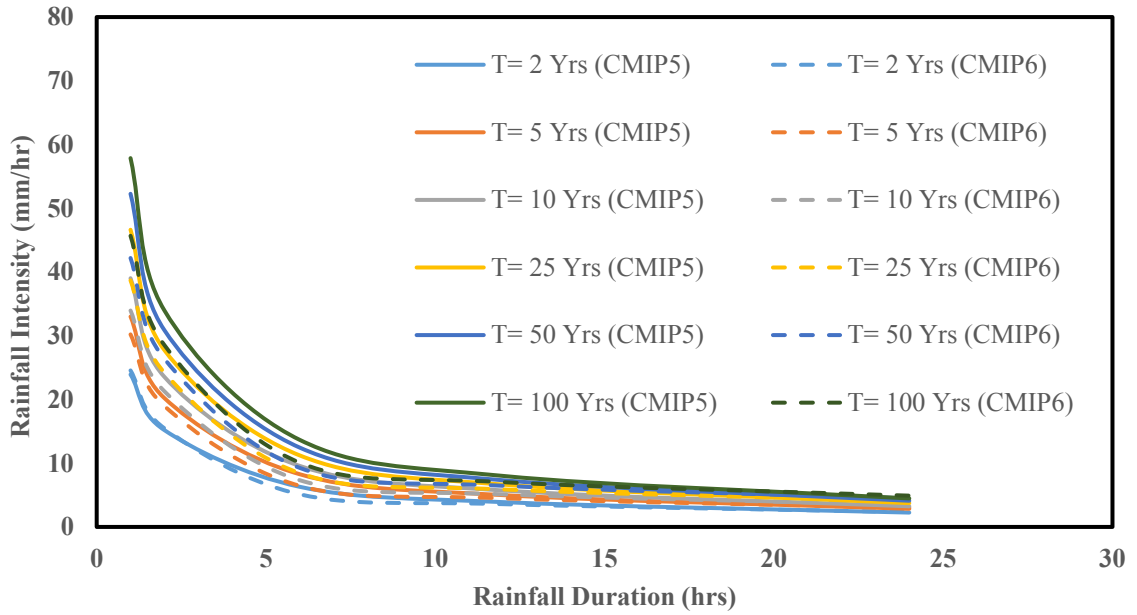


Figure 14. IDF curves for the near future period (TS-2: 2020–2059) considering a 2, 5, 10, 25, 50, and 100-year return period ensembling three CMIP5 RCP8.5 vs. CMIP6 SSP585 models

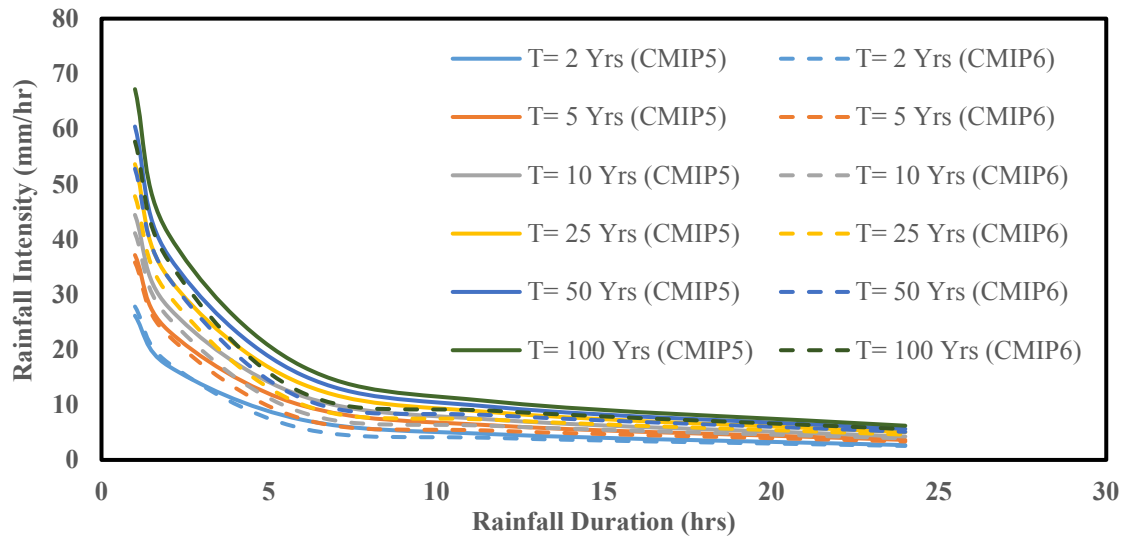


Figure 15. IDF curves for the far future period (TS-3: 2060–2099) considering a 2, 5, 10, 25, 50, and 100-year return period ensembling three CMIP5 RCP8.5 vs. CMIP6 SSP585 models

Chapter 3: Recommendations

Over the 21st century, it is highly probable that climate change will have a discernible impact on the distribution and intensity of rainfall. This, in turn, raises concerns about the capacity of our water drainage systems to cope with the anticipated surge in intense precipitation. The aim of this research work was to establish the relationship between intensity, duration, and frequency on an hourly scale using the CMIP5 and CMIP6 climate models under various climate change scenarios. Furthermore, the IDF curves generated from CMIP5 models for RCP8.5 and from CMIP6 for scenario SSP585 were analyzed and compared. The IDF curve was developed and extended to a temporal scale of one hour using simulated precipitation data for historical and future periods from climate models.

However, this study has limitations and suggests some directions for future studies. This is because the use of a limited number of models and scenarios may not represent the full range of uncertainty in the future. For example, future research is needed to incorporate several GCMs to understand the combined effects of these uncertainties with other sources of variability, such as land use change, natural internal weather variability, lake-atmosphere-land interaction, and so on. GCMs and RCMs both produce results with significant uncertainty, which calls attention to the necessity for uncertainty analysis and probability-based IDF curves. The climate model bias correction procedure has its own limitations. Future-period data that has been adjusted for bias uses the assumption that the bias is the same as the bias in the control period, which may not always be the case and may thus affect the results of the corrected data. Therefore, the design process should incorporate new ways to deal with and quantify uncertainty in the event of analyzing the effects of climate change. Despite these shortcomings, the study provides useful data for

city planners, engineers, and decision-makers to reduce the devastating effects of floods in the Town of Willoughby through the implementation of long-term, sustainable flood control measures.

In conclusion, the research highlights the significance of updating the current IDF curves, which might be helpful for the design of water management infrastructure to account for the consequences of climate change. There is a pressing need to review and update the IDF curve for the future, as the effects of climate change have already been noticed in this region. Further study can be conducted to incorporate several GCMs and conduct uncertainty analysis to report the lower and upper bounds of the IDF curve. In order to create a more resilient infrastructure system against climate change, state and federal agencies need to incorporate the future IDF curve in the design.